

Cite this: DOI: 10.1039/c2dt11954d

www.rsc.org/dalton

Ring-opening polymerisation of *rac*-lactide mediated by cationic zinc complexes featuring P-stereogenic bisphosphinimine ligands†

Hongsui Sun, Jamie S. Ritch and Paul G. Hayes*

Received 17th October 2011, Accepted 19th December 2011

DOI: 10.1039/c2dt11954d

The diastereomerically pure P-stereogenic bis(phosphinimine) ligands 4,6-(ArN=PMePh)₂dbf [Ar = 4-isopropylphenyl (Pipp): *rac*-**4**, *meso*-**4**; Ar = 2,6-diisopropylphenyl (Dipp): *rac*-**4a**; dbf = dibenzofuran] were synthesised and complexed to zinc using a protonation-alkane elimination strategy. The cationic alkylzinc complexes thus obtained, RZn[4,6-(ArN=PMePh)₂dbf][B(Ar')₄] [Ar = Pipp, Ar' = C₆H₃(CF₃)₂: *rac*-**6** (R = Et), *meso*-**6** (R = Et), *rac*-**7** (R = Me) *meso*-**7** (R = Me); Ar = Dipp: *rac*-**6a** (R = Et, Ar' = C₆H₃(CF₃)₂), *rac*-**6b** (R = Et, Ar' = C₆F₅)] were investigated for their competency as initiators for the ring-opening polymerisation of *rac*-lactide. The formation of polylactide was achieved under relatively mild conditions (40 °C, 2–4 h) and the microstructures of the resulting polymers exhibited a slight heterotactic bias [polymer tacticity (*P_r*) = 0.51–0.63].

Introduction

Bioplastics produced from plant sources continue to gain momentum as an alternative to petroleum-derived materials because of their renewability and biodegradability, as well as the rising cost of crude oil. One such biomaterial, polylactide (PLA), can be generated by the ring-opening polymerisation (ROP) of lactide. Although PLA is not yet commercially cost-competitive with traditional polyolefin plastics, it has found a growing number of niche applications. For example, its optical transparency and ease of processability render it suitable for food containers and packaging.¹ In addition, PLA has also been used by the medical community as a scaffold for tissue engineering and drug delivery systems.²

A widely-used industrial catalyst for PLA synthesis is bis(2-ethylhexanoate)tin(II), also known as tin(II) octanoate.³ Although this compound, as well as other metal alkoxides, can efficiently initiate the ROP of lactide, significant challenges in the development of new and improved catalysts still exist. To address some of these objectives, which include increasing activity and stereoselectivity, many single-site catalysts have been developed that possess modular ancillary ligands useful for tuning the steric and electronic properties of the metal complex.⁴ Many different metals, representing all blocks of the periodic table, have been used. Of particular interest to our group are inexpensive, non-toxic metals such as Ca, Mg and Zn,⁵ as such catalysts would not contaminate the resultant PLA with toxic transition metal ions.

The vast majority of ancillary ligands utilized in PLA synthesis are anionic, such as β-diketiminates,⁶ tethered alkoxides⁷ or tris(pyrazolyl)borates,⁸ and are used to support neutral metal complexes. We, however, have become interested in the ROP of lactide catalysed by *cationic* metal complexes featuring a *neutral* ancillary ligand, as little is known about such systems.⁹ Furthermore, cationic, coordinatively and electronically unsaturated metal complexes are expected to encourage facile coordination of LA. Correspondingly, we recently reported Mg¹⁰ and Zn¹¹ complexes of ligands featuring a dibenzofuran (dbf) framework with either one or two phosphinimine functionalities at the 4- and/or 6- positions (Chart 1). Rather than the metathetical route usually employed to introduce anionic ligands, we installed these neutral donors *via* a protonation-alkane elimination strategy whereby the ligand is protonated with an appropriate Brønsted acid to generate an aminophosphonium salt. This compound can then undergo an alkane elimination reaction upon exposure to organometallic reagents, such as ZnEt₂, to directly produce the desired cationic complex.

Lactide possesses two chiral centres, and hence the resultant polymers may feature different stereochemical arrangements depending on which form of the monomer is used: (*R,R*)-, (*S,S*)- or *meso*-lactide (Fig. 1). Physical properties, such as glass transition temperature, melting point and mechanical strength are

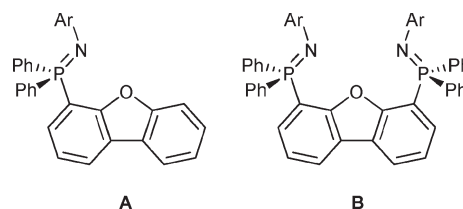


Chart 1 Two dibenzofuran-based ligands.

Department of Chemistry and Biochemistry, University of Lethbridge, 4401 University Drive, Lethbridge, AB, Canada, T1K 3M4. E-mail: p.hayes@uleth.ca; Fax: +1-403-329-2057; Tel: +1-403-329-2313

† Electronic supplementary information (ESI) available: Additional kinetic plots for complexes *rac*-**6** and *meso*-**6**. CCDC reference numbers 849079–849088. For ESI and crystallographic data in CIF or other electronic format see DOI: 10.1039/c2dt11954d

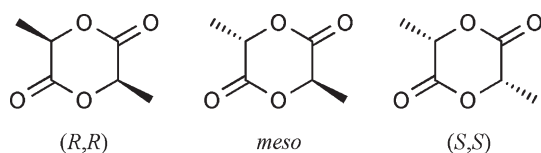


Fig. 1 Lactide stereoisomers.

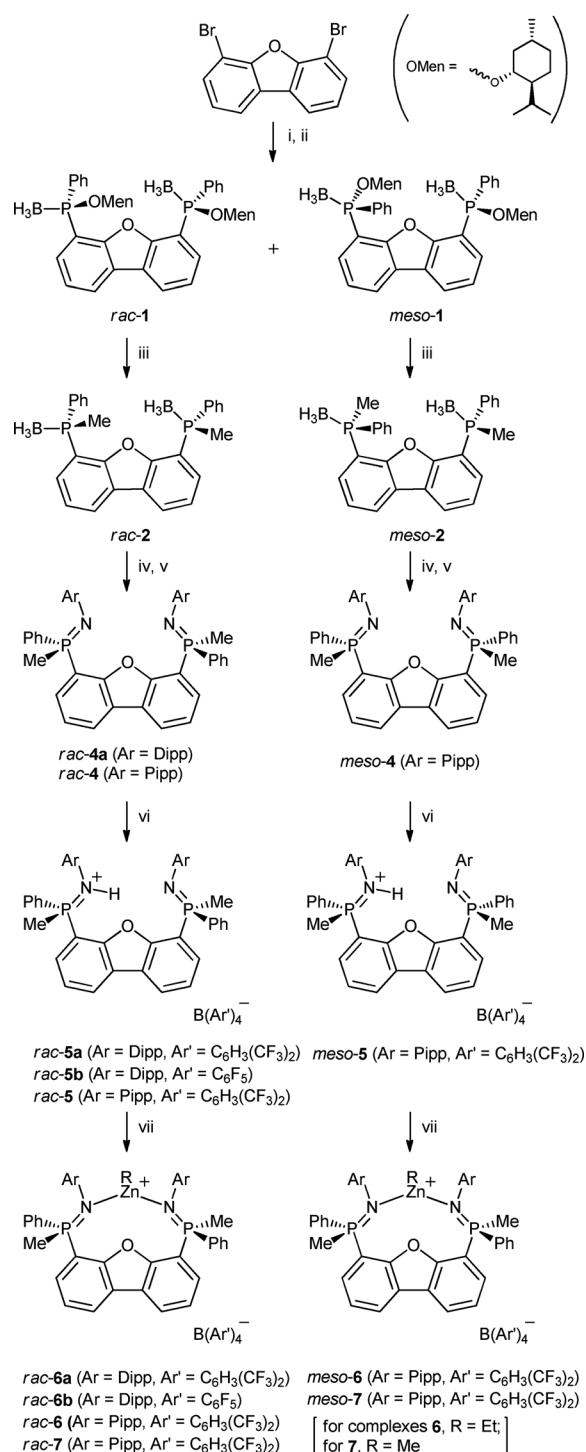
highly dependent on the degree of crystallinity, which in turn depends on the distribution of stereocentres in the polymer chains. Thus, stereochemically-controlled polymerisation of lactide has become an important concern.⁴ In particular, the synthesis of isotactic or heterotactic PLA from racemic lactide (*rac*-lactide, a 1 : 1 mixture of (*R,R*) and (*S,S*) forms), which allows for the formation of crystalline, high-melting polymers¹² without the need for resolution of the lactide starting material into enantiopure form, is a desirable objective. Achieving such stereoselectivity is nontrivial, however, as two independent processes affect the outcome of coordination-insertion polymerisations. The most prevalent of these two mechanisms is chain-end control, in which the stereochemistry of the last-inserted monomer influences the subsequent insertion. The other process is known as enantiomorphic site-control, and occurs when the absolute configuration of the catalyst affects each insertion step. Notably, these mechanisms are not necessarily mutually exclusive, and therefore, may compete with each other in a given reaction, with one or the other proving dominant for a particular catalyst system.¹³

Given the dramatic influence that polylactide microstructure has on the macroscopic properties of the resultant material it is not surprising that there is a growing interest in the synthesis of catalysts for stereoselective polymerisation of lactide. Dijkstra, Du and Feijen have recently reviewed advances in this area.⁴ Our plan to contribute to this area of research is to use our existing phosphinimine-functionalized dibenzofuran framework **B**, and engender chirality at the phosphorus centres by replacing one of the phenyl groups of the PPh₂ moiety with a methyl group. As a first step towards this goal, we recently reported the synthesis of several *P*-stereogenic monophosphinimine analogues of **A** and their complexes, [$\{(\text{dbf})\text{MePhP}=\text{NAr}\}\text{ZnR}\}\text{[B(C}_6\text{F}_5)_4\text{]}$ (Ar = Dipp, Mes (2, 4, 6-trimethylphenyl); R = Et, methyl-(*S*)-lactate), and investigated their activity in the synthesis of PLA.¹⁴ These complexes were found to initiate the ROP of lactide, but the activity was relatively low ($T = 80^\circ\text{C}$, 9 h), and no stereochemical preference was observed in the resulting polymers ($P_r = ca. 0.5$). Inspired by our previous work, in which it was established that bisphosphinimine dbf-based ligands elicit substantially higher activity than their monofunctionalized counterparts **A**,^{11b,c} we now describe the synthesis of cationic alkylzinc complexes supported by pincer ligands featuring *two* chiral phosphinimine donors.

Results and discussion

Ligand synthesis and metal complexation

The syntheses of the desired 4,6-disubstituted ligands (Scheme 1) started with 4,6-dibromodibenzofuran. This strategy differs from the synthesis of the singly-substituted ligands (dbf)



Scheme 1 Synthetic route to the cationic zinc complexes **6** and **7**. i: 2 *n*-BuLi, (OMen)PhPCl; ii: BH₃·THF; iii: MeLi; iv: HNEt₂; v) ArN₃; vi) [H(Et₂O)₂][BAR'₄]; vii) ZnR₂. For clarity, only one stereoisomer is shown for the *rac*-compounds.

MePhP=NAr (Ar = Dipp, Mes),¹⁴ whereby the first step was lithiation of dibenzofuran with *n*-BuLi, followed by reaction with (OMen)PPhCl (OMen = (–)-*O*-menthyl) and subsequently BH₃·THF to afford the intermediate (OMen)(dbf)PhP(BH₃). When this approach was employed using 1,8-dilithiodibenzofuran,¹⁵ the subsequent reaction with two equiv of

chlorophosphine yielded a mixture of free dibenzofuran, $(\text{dbf})_2\text{PhP}(\text{BH}_3)$ and $(\text{OMen})_2\text{Ph}(\text{BH}_3)$ along with a small quantity of the desired product. A more efficient method for generating the requisite 1,8-dilithiodibenzofuran was accomplished by a lithium halogen exchange reaction in which 1,8-dibromodibenzofuran was allowed to react with 2 equiv of $^t\text{BuLi}$ at -78°C in THF solution. After 2 h, the reaction mixture was treated with $\text{BH}_3\cdot\text{THF}$, affording a crude product containing three borane protected diastereomers, 4,6- $\{(\text{OMen})\text{PhP}(\text{BH}_3)\}_2(\text{dbf})$ (*rac*-**1**: (*R,R,R,R*) + (*R,S,S,R*) and *meso*-**1**: (*R,S*)). \ddagger Flash chromatography using benzene/hexanes (1 : 4) as the eluent on silica gel allowed for separation of the *rac* and *meso* isomers to give analytically pure crystalline, colourless products in 33 and 26% yield, respectively. Although we were unable to fully separate the two *rac* stereoisomers, this still represents a significant advancement for our dbf-based systems, as diastereomeric resolution was not possible with the monophosphine analogues; exhaustive attempts using a range of experimental conditions, consistently resulted in elution of the two diastereomers as an inseparable mixture.¹⁴ The successful separation in this study allowed more detailed characterisation of these diastereomers. To this end, X-ray quality single crystals of *rac*-**1** and *meso*-**1** were obtained and their absolute configurations were confirmed by X-ray diffraction studies (*vide infra*). Interestingly, the (*R,R,R,R*) and (*R,S,S,R*) forms of *rac*-**1** were distinguishable by ^1H NMR spectroscopy, as two separate mentholate OCH resonances were observed in a 31 : 69 ratio; unique signals for this group were also observed in the $^{13}\text{C}\{^1\text{H}\}$ NMR spectrum. These data indicate that *rac*-**1** was partially resolved with a slight diastereomeric excess (38%) in favour of either (*R,R,R,R*) or (*R,S,S,R*) configurations at phosphorus. The *meso* isomer only exhibited one ^1H OCH environment due to signal broadness; however, two sets of OCH resonances were clearly distinguishable in the $^{13}\text{C}\{^1\text{H}\}$ NMR spectrum.

When *rac*-**1** was subject to recrystallization from benzene/pentane, a single crystal was selected and determined to be a disordered mixture of the two stereoisomers (*R,S,S,R*)-**1** (major) and (*R,R,R,R*)-**1** (minor). Upon successive recrystallizations, the bulk sample became increasingly enriched with (*R,S,S,R*)-**1**, which suggests that this is the stereoisomer in excess in the initial product, and that the diastereomeric excess arises from preferential crystallization. Suitable crystals of the *meso* form of **1** were also obtained and structurally characterised, which confirmed the expected connectivity. Efforts to fully resolve the (*R,R,R,R*) and (*R,S,S,R*) stereoisomers have thus far been unsuccessful.

Removal of the OMen resolving groups was achieved by the facile reaction of **1** with MeLi in benzene at 40°C to generate the products 4,6- $\{\text{MePhP}(\text{BH}_3)\}_2(\text{dbf})$ (*rac*-**2** and *meso*-**2**) in 59 and 51% yields, respectively. Once again, crystalline products were obtained. In the case of *rac*-**2**, when the reaction was conducted at ambient temperature, the partially methylated by-product 4- $\{\text{MePhP}(\text{BH}_3)\}$ -6- $\{(\text{OMen})\text{PhP}(\text{BH}_3)\}(\text{dbf})$ (**3**) was also obtained in the reaction mixture in 10% yield. This compound, formed due to incomplete conversion at ambient temperature, was purified and independently characterized (see Experimental section for details). The methylated compounds *rac*- and *meso*-**2** exhibited ^{31}P NMR chemical shifts of δ 9.08 and 9.27, respectively. *Rac*-**2** crystallized as a racemic mixture

(1 : 1) of two enantiomers, and hence no preferential crystallization of one stereoisomer was observed.

Removal of the borane protecting groups from **2** by heating in neat diethylamine, followed by assembly of the phosphinimine functionalities under standard Staudinger conditions,¹⁶ was performed to yield neutral ligands in one-pot: 4,6- $\{\text{MePhP}=\text{NAr}\}_2(\text{dbf})$ (Ar = Dipp: *rac*-**4a**; Ar = Pipp (4-isopropylphenyl): *rac*-**4** and *meso*-**4**). These compounds were obtained as analytically pure solids. Upon deprotection and installation of the NAr moieties, a shielding effect was observed in the resulting complexes (^{31}P : δ -15.21 for *rac*-**4a** and δ -2.26 to -2.07 for *rac*- and *meso*-**4**). One of the neutral ligands, *rac*-**4a**, was also subjected to X-ray diffraction analysis, revealing P=N bond lengths of 1.551(1) Å and 1.547(1) Å. These values closely match those observed in the related ligand 4,6-(MesN=PPh₂)₂dbf (1.549(1) Å and 1.565(1) Å).^{11a}

The ligands **4** were easily protonated with the Brønsted acids $[\text{H}(\text{Et}_2\text{O})_2][\text{BAR}'_4]$ (Ar' = $\text{C}_6\text{H}_3(\text{CF}_3)_2$, C_6F_5) to give the corresponding aminophosphonium salts $[\text{H-4,6-}\{\text{MePhP}=\text{NAr}\}_2(\text{dbf})][\text{BAR}'_4]$ (Ar = Dipp: *rac*-**5a** (Ar' = $\text{C}_6\text{H}_3(\text{CF}_3)_2$), *rac*-**5b** (Ar' = C_6F_5); Ar = Pipp, Ar' = $\text{C}_6\text{H}_3(\text{CF}_3)_2$: *rac*-**5**, *meso*-**5**) as white crystalline solids. The protonated ligands **5** exhibit $^{31}\text{P}\{^1\text{H}\}$ NMR spectra with single resonances at δ 9.17–9.20 for Dipp-substituted compounds, and δ 15.20–15.84 for the Pipp-containing analogues; the presence of single ^{31}P NMR resonances for these compounds suggests that, on the NMR timescale in solution, the NH proton is rapidly exchanging between the two phosphinimine groups. The ^1H signal for this proton was observed at *ca.* δ 4.8 (Ar = Dipp) and 6.4 (Ar = Pipp). Upon protonation, the P=N distances elongated by approximately 5% to 1.624(2) Å and 1.619(3) Å as seen in the structures of *rac*-**5a** and *rac*-**5b**, respectively. The other moieties in these compounds remain relatively unchanged, and in the solid state the proton is localized on one phosphinimine group, rather than shared between the two.

The reaction of these salts with ZnMe_2 or ZnEt_2 furnished the desired cationic organozinc complexes $\text{RZn}[4,6-(\text{ArN}=\text{PMePh})_2\text{dbf}][\text{B}(\text{Ar}'_4)]$ [Ar = Dipp: *rac*-**6a** (R = Et, Ar' = $\text{C}_6\text{H}_3(\text{CF}_3)_2$), *rac*-**6b** (R = Et, Ar' = C_6F_5); Ar = Pipp, Ar' = $\text{C}_6\text{H}_3(\text{CF}_3)_2$: *rac*-**6** (R = Et), *meso*-**6** (R = Et), *rac*-**7** (R = Me), *meso*-**7** (R = Me)] via alkane elimination. The various alkylzinc complexes **6** and **7** all feature ^{31}P environments which resonate in the narrow range of δ 24.49–25.71, indicating the electronic effect that the coordinated metal centre has on P dominates over the influence from the different aryl substituents on nitrogen. These chemical shifts agree well with similar complexes, *e.g.* the ^{31}P NMR chemical shift for the achiral complex $\text{MeZn}[4,6-(\text{MesN}=\text{PPh}_2)_2\text{dbf}][\text{B}(\text{C}_6\text{F}_5)_4]$ appears at δ 23.4 in $\text{C}_6\text{D}_5\text{Br}$ at ambient temperature.^{11b} The $^{11}\text{B}\{^1\text{H}\}$ and $^{19}\text{F}\{^1\text{H}\}$ NMR signals for the borate anions in the zinc complexes **6** and **7** and the protonated ligands **5** were unremarkable and consistent with symmetrical, weakly coordinating fragments in solution. Essentially no change in δ was observed between the protonated ligands and their corresponding zinc alkyl complexes.

In our previous work, we have found that alkyl substituents on zinc are poorer initiating groups when compared to methyl-(*S*)-lactate.^{11c} However, the reaction of the protonated ligands **5** with $\text{EtZn}(\text{methyl-}(S)\text{-lactate})$,¹⁷ EtZnO^iPr or reactions of the zinc complexes **6** and **7** with methyl-(*S*)-lactate gave

intractable mixtures of products. Therefore, polymerisation studies were conducted using the alkylzinc complexes (*vide infra*). Further experiments are currently underway to form alkoxy and amido-substituted zinc complexes.

X-ray crystal structures of three alkylzinc complexes (*rac*-**6a**, *meso*-**6** and *meso*-**7**) were obtained (CIF data can be found in the ESI†). In all three cases, no strong cation–anion interactions were observed [shortest cation–anion contacts were aromatic C_{cation}–F_{anion} distances: *rac*-**6a** (2.93 Å), *meso*-**6** (3.02 Å), and *meso*-**7** (3.04 Å), *cf.* sum of van der Waals radii = 3.17^{18a}] and the coordination geometry at zinc was found to be essentially trigonal planar ($\Sigma(\text{Zn}) = \text{ca. } 357.9\text{--}359.94^\circ$); no significant interactions with the dbf oxygen atoms were observed ($d(\text{Zn}\cdots\text{O}) = \text{ca. } 2.9\text{--}3.4$ Å).

This finding lies in contrast to complexes recently reported by our group, $\text{MeZn}[4,6\text{-(PippN=PPh}_2)_2\text{dbf}][\text{BPh}_4]$,^{11c} (methyl-*S*-lactate) $\text{Zn}[4,6\text{-(PippN=PPh}_2)_2\text{dbf}][\text{BPh}_4]$ ^{11c} and (methyl-*S*-lactate) $\text{Zn}[4,6\text{-(PhN=PPh}_2)_2\text{dbf}][\text{B}(\text{C}_6\text{H}_3(\text{CF}_3)_2)]$ ^{11d} where clear Zn \cdots O interactions (2.284(2), 2.336(5) and 2.367(2) Å, respectively) were found in the solid state. Notably, the methyl-*S*-lactate complex was found to be a very active catalyst for the polymerisation of *rac*-lactide. This compound exhibits a significant Zn \cdots O interaction (with a distance in between the sums of the covalent radii and van der Waals radii of 1.90^{18b} and 2.91 Å,^{18a} respectively), that is perhaps a reflection of a greater effective positive charge on the zinc centre or more open coordination sphere. Either of these factors would be expected to aid in a coordination-insertion type polymerisation mechanism. The fact that no such interaction was seen for *rac*-**6a**, *meso*-**6** or *meso*-**7** is a potential indicator that they will not be as effective in lactide polymerisation catalysis.

The structure of *meso*-**6** is depicted in Fig. 2. Interestingly, in *rac*-**6a** the ligand is pseudo-*C*₂ symmetric, with two phosphinimine groups coordinated to the metal centre in an *anti* fashion (one above the plane of the dbf ligand and one below), while for the *meso* complex a *syn*-coordination is seen, giving a pseudo-*C*_s symmetric cation. This difference is presumably due to the presence of the larger Dipp groups in *rac*-**6a**, which would be in

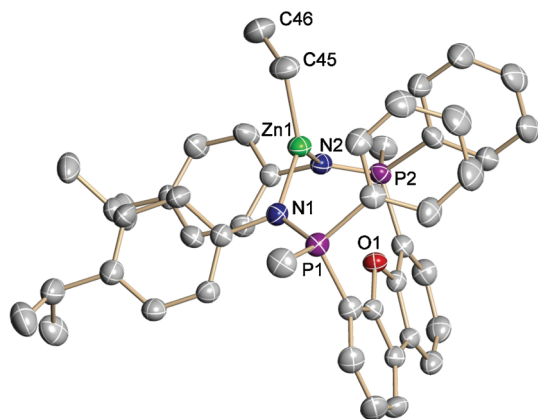


Fig. 2 Thermal ellipsoid plot (50% probability) of *meso*-**6**; hydrogen atoms and the $[\text{B}(\text{C}_6\text{H}_3(\text{CF}_3)_2)_4]^-$ anion are omitted for clarity. Selected bond lengths (Å) and angles ($^\circ$): Zn1–N1 2.037(3), Zn1–N2 2.038(3), Zn–C45 1.976(4), N1–P1 1.601(3), N2–P2 1.594(3); N1–Zn1–N2 115.2(1), N1–Zn1–C45 123.5(1), C45–Zn1–N2 119.8(1).

close proximity to each other in the *syn* geometry. The smaller Pipp substituents allow access to this coordination mode for *meso*-**6** and *meso*-**7**. The Zn–N distances in these complexes range from 2.028(2)–2.038(3) Å for the *meso* complexes, and 2.061(3)–2.063(3) Å for *rac*-**6a**. These are in excellent agreement with the values of 2.033(4)–2.044(4) Å determined for the complex $\text{MeZn}[4,6\text{-(MesN=PPh}_2)_2\text{dbf}][\text{BPh}_4]$.^{11b} The slightly elongated values in the *rac* complex are attributed to the larger Dipp substituents on nitrogen, which cause steric crowding around the metal centre.

Polymerisation studies

The Dipp-substituted compounds *rac*-**6a** and *rac*-**6b** were not active catalysts for the ROP of *rac*-lactide, presumably due to the steric bulk of the Dipp groups on nitrogen. We note that similarly inactive complexes were obtained with mesityl-substituted bis-(phosphinimine)dbf ligands.^{11b} By comparison, the less bulky Pipp-substituted complexes showed much more promise in this area. Thus, in order to ascertain the influence of stereochemistry at phosphorus on the polymerisation chemistry of the corresponding metal complexes, the two Pipp-substituted compounds *rac*-**6** and *meso*-**6** were used in the ROP of *rac*-lactide. Despite the absence of methyl-(*S*)-lactate initiating groups on zinc, both complexes appeared to be competent ROP initiators. In fact, the activity of these compounds was substantially higher than that previously reported for the monophosphinimine complex (methyl-(*S*)-lactate) $\text{Zn}[4\text{-(DippN=PMePh)dbf}][\text{B}(\text{C}_6\text{F}_5)_4]$.¹⁴ Using NMR-scale reactions in CDCl_3 , conditions for larger scale polymerisations were determined. Excellent yields were obtained for the solid polymers, which were then analysed by triple-detection GPC (Table 1).

At higher loadings, the M_n values were much larger than calculated for both initiators; this was also true for the lowest loading of *meso*-**6**. All of the M_w values were significantly higher than corresponding M_n values which is reflected in the relatively large polydispersity indices (PDI: 1.69–2.62). No other clear trends in the molecular weight data are apparent. However, the data do suggest significant transesterification processes and/or initiator degradation occurred during polymerisation, leading to larger than expected chains of polylactide (*i.e.* if fewer active sites are present in solution, the propagating chains will be longer than calculated). Analysis by MALDI-TOF mass spectrometry yielded further information on the polymer chain structure. For samples prepared using *rac*-**6** or *meso*-**6**, ions corresponding to the formulae $[\text{H}(\text{C}_6\text{H}_8\text{O}_4)_n\text{OH}] + \text{Na}^+$ were identified, with molecular weights for these ions ranging from *ca.* 1000 to >7000 amu. Spacings of 72 amu between ions were also apparent, suggesting significant transesterification occurs during polymerisation. Monitoring the polymerization reactions *in situ* by NMR spectroscopy yielded no further insight into such a process.

The hydroxy-terminated nature of the obtained polymers (*i.e.* the lack of ethyl end groups) suggests that *rac*-**6** and *meso*-**6** are not true catalysts, but rather, first undergo preliminary reactions to form the actual active species. This has been suggested for the industrial catalyst tin(II) octanoate.⁴ A cationic zinc hydroxy species may be a reasonable candidate for the true active species,

Table 1 GPC results for polylactide samples prepared using *rac*-6 and *meso*-6^a

Initiator	[LA] ₀ /[Zn]	Isolated yield (%)	Time (h)	Calc. $M_n (\times 10^3)$	$M_n (\times 10^3)$	$M_w (\times 10^3)$	PDI
<i>rac</i> -6	200	97.2	2.0	28.0	93.4	165.2	1.77
<i>rac</i> -6	400	98.6	2.7	56.8	102.5	172.9	1.69
<i>rac</i> -6	600	97.2	3.3	84.1	38.3	70.7	1.85
<i>rac</i> -6	800	92.9	3.7	107.1	65.5	111.8	1.71
<i>rac</i> -6	1000	89.6	4.0	129.1	56.3	96.5	1.71
<i>meso</i> -6	200	99.3	2.0	28.6	87.0	187.1	2.15
<i>meso</i> -6	400	98.2	2.5	56.6	71.7	188.1	2.62
<i>meso</i> -6	600	99.9	3.2	86.4	60.5	120.0	1.98
<i>meso</i> -6	800	97.7	3.5	112.7	89.2	211.9	2.38
<i>meso</i> -6	1000	95.3	3.8	137.4	208.3	390.7	1.87

^a Experimental conditions: methylene chloride, 40 °C, samples precipitated from cold methanol and dried *in vacuo*.

Table 2 The influence of solvent on polymer tacticity^a

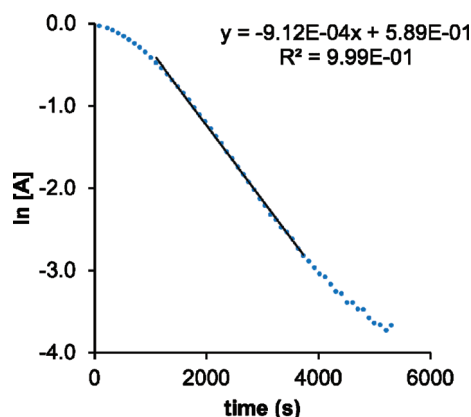
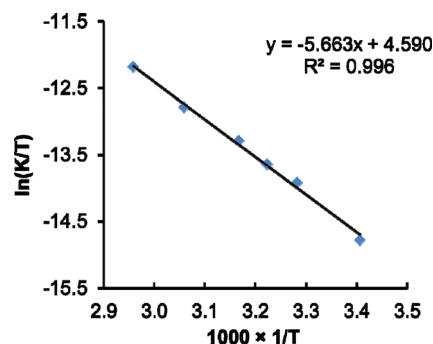
Initiator	P_r (THF- <i>d</i> ₈)	P_r (CDCl ₃)	P_r (Benzene- <i>d</i> ₆)
<i>rac</i> -6	0.63	0.62	0.52
<i>meso</i> -6	0.57	0.51	0.56

^a Experimental conditions: 25 °C, 15 h. ¹H{¹H} NMR spectra recorded on isolated polymer samples that were redissolved in CDCl₃.

although we have thus far been unable to independently prepare such a complex. Current efforts are underway to synthesize alkoxyzinc analogues of *rac*-6 and *meso*-6 in order to compare their structure and catalytic activities. Overall, the mechanism of polymerisation remains unclear. *In situ* ³¹P{¹H} and ¹H NMR experiments were complex and yielded no conclusive data on, e.g. coordination-insertion events.

The microstructure of the polymer samples was probed by homodecoupled ¹H{¹H} NMR spectroscopy. Upon examination of the methine region, values of P_r were obtained for polymers made using *rac*-6 and *meso*-6 as initiators and in several different solvents (Table 2). Overall, a modest bias was observed for heterotacticity ($P_r = 0.52$ – 0.63 for *rac*-6 and 0.51 – 0.57 for *meso*-6), indicating some form of chain-end control¹³ is occurring during the polymerisation, but it is clearly not a strong effect. Nonetheless, a significant improvement is seen when compared with the monophosphinimine variants, which yielded entirely atactic samples.¹⁴

Kinetic data were collected using both complexes at various temperatures. A plot of the natural logarithm of the monomer concentration *versus* time for *rac*-6 is depicted in Fig. 3, and is representative of other kinetic runs. A noticeable induction period precedes the linear regime in these reactions, which are first order in [monomer]. Eyring and Arrhenius plots (Fig. 4 displays the Eyring plot for *rac*-6; refer to ESI† for other plots) allowed for extraction of activation parameters. The complex *rac*-6 yielded values of $\Delta H^\ddagger = 47.1 \pm 1.5 \text{ kJ mol}^{-1}$, $\Delta S^\ddagger = -159 \pm 4.9 \text{ J K}^{-1} \text{ mol}^{-1}$, and $E_a = 49.7 \pm 1.5 \text{ kJ mol}^{-1}$, while *meso*-6 gave $\Delta H^\ddagger = 39.1 \pm 3.3 \text{ kJ mol}^{-1}$, $\Delta S^\ddagger = -197 \pm 10.5 \text{ J K}^{-1} \text{ mol}^{-1}$, and $E_a = 41.7 \pm 3.3 \text{ kJ mol}^{-1}$. Such data are consistent with an ordered transition state, and match well with values previously reported for coordination-insertion mechanisms,¹⁹ although the exact steps of polymerisation in this system are as of yet unknown.

**Fig. 3** Plot of $\ln[A]$ *versus* t for polymerisation using *rac*-6 at 50 °C.**Fig. 4** Eyring plot [$\ln(K/T)$ *versus* $1000 \times 1/T$] for complex *rac*-6.

Experimental

Reagents and general procedures

Manipulations of air- and moisture-sensitive materials and reagents were carried out under an argon atmosphere using vacuum line techniques or in a glove box. Solvents used for air-sensitive materials were purified using an MBraun solvent purification system (SPS), stored in PTFE-sealed glass vessels over sodium benzophenone ketyl (THF and ether), CaH₂ (CH₂Cl₂ and bromobenzene) or “titanocene” (pentane, benzene and toluene), and freshly distilled at the time of use. Deuterated solvents were dried over sodium benzophenone ketyl (benzene-*d*₆

and THF-*d*₈) or CaH₂ (CDCl₃ and CD₂Cl₂), degassed *via* three freeze–pump–thaw cycles, distilled *in vacuo* and stored over 4 Å molecular sieves in glass bombs under argon. NMR spectra were recorded at ambient temperature with a Bruker Avance II NMR spectrometer (300.13 MHz for ¹H, 75.47 MHz for ¹³C, 121.48 MHz for ³¹P, 282.42 MHz for ¹⁹F and 96.29 MHz for ¹¹B). Chemical shifts are reported in parts per million relative to the external standards SiMe₄ (¹H), 85% H₃PO₄ (³¹P), trifluorotoluene (¹⁹F) and boron trifluoride diethyl etherate (¹¹B); residual H-containing species in CD₂Cl₂ (δ 5.32 ppm) or CDCl₃ (δ 7.27 ppm) were used as internal references (¹H). Assignments were aided by the use of ¹³C{¹H}-DEPT and ¹H-¹³C{¹H}-HSQC experiments (s = singlet, d = doublet, t = triplet, q = quartet, sp = septet, m = multiplet, br = broad, ov = overlapping signals). Elemental analyses were performed using an Elementar Vario Microcube instrument. The reagents 2,6-dibromodibenzofuran,²⁰ (OMen)PhPCl (OMen = (–)-menthyl),¹⁴ [H(Et₂O)₂]-[B(C₆H₃{CF₃})₂]₄,²¹ [H(Et₂O)₂][B(C₆F₅)₄],²² DippN₃²³ and PippN₃,²⁴ and *S*-MeO₂CC(H)(Me)OZnEt¹⁷ were prepared according to literature methods. *Rac*-lactide was purchased from Alfa Aesar and purified by double recrystallization from toluene followed by sublimation. Diethylamine (Aldrich) was dried over 4 Å molecular sieves and degassed prior to use. All other reagents were purchased from commercial sources and used as received. Flash chromatographic purification was run on silica gel (230–400 mesh, as received and without activation) using a fritted column (3 × 45 cm). GPC data were collected on a Viscotek Triple Detection GPC System outfitted with a model 270 Dual Detector Platform (Four Capillary Viscometer and Light Scattering Detector) and a Refractive Index Detector. Samples were run in THF at a concentration of 1 mg mL^{–1}. MALDI-TOF data were collected using an Applied BioSystems Voyager Elite instrument.

Synthesis of *rac*-1 and *meso*-1

Dibromodibenzofuran (5.0 g, 15.3 mmol) was dissolved in THF (*ca.* 100 mL) and cooled to –78 °C. To the well-stirred solution *n*-BuLi (19.6 mL, 31.4 mmol, 1.6 M in hexane) was added dropwise. The light brown solution became deeper in colour and precipitates were observed to form. The suspension was stirred at –78 °C for 1 h, followed by an additional 1 h at 0 °C. The resulting suspension was cooled to –78 °C again and (–)-(*O*-menthyl)chlorophenylphosphine (9.38 g, 31.3 mmol) in THF (20 mL) was added dropwise. The mixture was left to warm to ambient temperature overnight, resulting in a light orange solution. At 0 °C, BH₃·THF (40 mL, 40 mmol, 1 M in THF) was slowly added and stirring was continued at ambient temperature for 1 h. To the resulting solution water (20 mL) was added. The organic layer was separated and the aqueous solution was extracted with hexanes (3 × 15 mL). The combined organic fractions were washed with brine and dried over MgSO₄. After removal of volatiles *in vacuo*, the residue was subjected to column separation. Upon elution with benzene/hexanes (1 : 4), *rac*-1 (3.6 g, 5.0 mmol, 33%) and *meso*-1 (2.9 g, 4.0 mmol, 26%) were obtained. After recrystallization of *rac*-1 from benzene/hexanes, the ratio of (*R,R,R,R*) to (*R,S,S,S*) had changed to 31 : 69, according to ¹H NMR spectroscopy. Single crystals of

rac-1 and *meso*-1 suitable for analysis by X-ray crystallography were prepared by dissolving samples in benzene in 5 mm diameter glass tubes and layering the solution with pentane.

A 31 : 69 ratio of *rac*-1:(*R,R,R,R*):(*R,S,S,S*) was determined experimentally; for simplicity data are listed as integrations for an ideal 1 : 1 racemic mixture. ¹H NMR (CDCl₃): δ 8.27–8.06 (m, 4H (*R,S,S,S*), 4H (*R,R,R,R*), 1,2,8,9-dbf), 7.65–7.17 (br ov m, 12H (*R,S,S,S*) and 12H (*R,R,R,R*), 3,7-dbf + Ph), 4.37 and 4.18 (br m, 2H (*R,S,S,S*) and 2H (*R,R,R,R*), OCH), 2.09–0.9 (ov m, 30H (*R,S,S,S*) and 30H (*R,R,R,R*), OMen + BH₃), 0.75 (d, ³*J*_{HH} = 6.2 Hz, 3H (*R,S,S,S*) and 3H (*R,R,R,R*), CHCH₃), 0.68 (d, ³*J*_{HH} = 6.2 Hz, 3H (*R,S,S,S*) and 3H (*R,R,R,R*), CHCH₃), 0.31 (d, ³*J*_{HH} = 6.6 Hz, 3H (*R,S,S,S*) and 3H (*R,R,R,R*), CHCH₃), 0.13 (d, ³*J*_{HH} = 6.6 Hz, 3H (*R,S,S,S*) and 3H (*R,R,R,R*), CHCH₃). ¹³C{¹H} NMR (CDCl₃): δ: (*R,S,S,S*) diastereomer, 155.95 (s, OC-dbf), 133.38 (s, 3/7-dbf), 133.36 (d, ¹*J*_{CP} = 73.2 Hz, 4,6-dbf), 131.41 (s, aromatic C), 130.84 (d, ²*J*_{CP} = 11.8 Hz, aromatic C), 128.69 (d, ²*J*_{CP} = 11.2 Hz, *o*-Ph), 125.10 (s, aromatic C), 123.99 (d, ³*J*_{CP} = 4.5 Hz, dbf), 123.25 (d, ²*J*_{CP} = 11.3 Hz, aromatic C), 117.09 (d, ¹*J*_{CP} = 58.1 Hz, Ph), 80.81 (d, ²*J*_{CP} = 2.6 Hz, POC-Men ring), 47.74 (d, ³*J*_{CP} = 5.3 Hz, CHCH(CH₃)₂), 43.54 (s, OCHCH₂CH), 34.34 (s, CH₃CHCH₂CH₂CH), 31.68 (s, CH₂CH(CH₃)CH₂), 25.21 (s, CHCH(CH₃)₂), 22.70 (s, CH₃CHCH₂CH₂CH), 22.38 (s, CH₂CH(CH₃)CH₂), 20.66 (s, CHCH(CH₃)₂), 14.93 (s, CHCH(CH₃)₂). (*R,R,R,R*) diastereomer, 156.18 (d, ²*J*_{CP} = 2.3 Hz, OC-dbf), 133.16 (s, 3/7-dbf), 132.42 (d, ¹*J*_{CP} = 73.2 Hz, 4,6-dbf), 131.85 (s, aromatic C), 131.10 (d, ²*J*_{CP} = 11.8 Hz, aromatic C), 128.46 (d, ²*J*_{CP} = 10.9 Hz, *o*-Ph), 124.56 (s, aromatic C), 124.24 (d, ³*J*_{CP} = 6.0 Hz, dbf), 123.22 (d, ²*J*_{CP} = 9.8 Hz, aromatic C), 118.03 (d, ¹*J*_{CP} = 60.4 Hz, Ph), 80.73 (d, ²*J*_{CP} = 2.7 Hz, POC-Men ring), 48.16 (d, ³*J*_{CP} = 6.8 Hz, CHCH(CH₃)₂), 42.75 (s, OCHCH₂CH), 34.09 (s, CH₃CHCH₂CH₂CH), 31.64 (s, CH₂CH(CH₃)CH₂), 25.63 (s, CHCH(CH₃)₂), 22.90 (s, CH₃CHCH₂CH₂CH), 22.19 (s, CH₂CH(CH₃)CH₂), 21.15 (s, CHCH(CH₃)₂), 15.61 (s, CHCH(CH₃)₂). ³¹P{¹H} NMR (CDCl₃): δ 99.86 (br s). ¹¹B{¹H} NMR (CDCl₃): δ –39.32 (br s). Anal. Calcd for C₄₄H₆₀B₂O₃P₂: C, 73.35; H, 8.39. Found: C, 73.48; H, 8.29.

meso-1: ¹H NMR (CDCl₃): δ 8.25–8.04 (ov m, 4H, 1,2,8,9-dbf), 7.75–7.69 (m, 2H, 3,7-dbf), 7.52–7.40 (ov m, 5H, Ph), 7.32–7.22 (ov m, 5H, Ph), 4.38 (m, 2H, POCH-Men ring), 2.03 (br m, 2H, OMen), 1.90 (br d, ³*J*_{HH} = 12.0 Hz, 1H, OMen), 1.71–1.03 (ov m, 17H, OMen + BH₃), 0.91 (ov t, ³*J*_{HH} = 7.0 Hz, 10H, OMen + BH₃), 0.74 (d, ³*J*_{HH} = 6.6 Hz, 6H, CH₃), 0.41 (d, ³*J*_{HH} = 6.6 Hz, 3H, CH₃), 0.36 (d, ³*J*_{HH} = 6.9 Hz, 3H, CH₃). ¹³C{¹H} NMR (CDCl₃): δ 156.30 (s, dbf-OC), 156.16 (s, dbf-OC), 133.04 (d, ²*J*_{CP} = 15.8 Hz, 3/7-dbf), 132.92 (d, ¹*J*_{CP} = 73.2 Hz, 4/6-dbf), 132.64 (d, ¹*J*_{CP} = 77.0 Hz, 4/6-dbf), 132.17 (d, ²*J*_{CP} = 12.1 Hz, 3/7-dbf), 132.08 (s, aromatic C), 131.81 (s, aromatic C), 131.73 (s, aromatic C), 131.48 (s, aromatic C), 131.32 (s, aromatic C), 130.81 (d, *J*_{CP} = 12.1 Hz, aromatic C), 128.68 (d, *J*_{CP} = 10.6 Hz, aromatic C), 128.35 (d, *J*_{CP} = 11.3 Hz, aromatic C), 124.98 (d, ²*J*_{CP} = 30.9 Hz, Ph), 124.26 (d, ³*J*_{CP} = 5.3 Hz, dbf), 124.13 (d, ³*J*_{CP} = 3.8 Hz, dbf), 123.44 (d, *J*_{CP} = 9.8 Hz, aromatic C), 123.20 (d, *J*_{CP} = 11.3 Hz, aromatic C), 117.56 (d, ¹*J*_{CP} = 61.1 Hz, Ph), 81.15 (d, ²*J*_{CP} = 3.0 Hz, POCH-Men ring), 80.65 (d, ²*J*_{CP} = 3.0 Hz, POCH-Men ring), 48.62 (d, ³*J*_{CP} = 6.8 Hz, CHCH(CH₃)₂), 48.25 (d, ³*J*_{CP} = 5.3 Hz, CHCH(CH₃)₂), 43.80 (s, OCHCH₂CH), 42.83 (s, OCHCH₂CH), 34.32

(s, CH₃CHCH₂CH₂CH), 34.22 (s, CH₃CHCH₂CH₂CH), 31.67 (s, CH₂CH(CH₃)CH₂), 31.60 (s, CH₂CH(CH₃)CH₂), 25.70 (s, CHCH(CH₃)₂), 25.62 (s, CHCH(CH₃)₂), 22.84 (s, CH₃CHCH₂CH₂CH, (2 coincident signals)), 22.33 (s, CH₂CH(CH₃)CH₂), 22.14 (s, CH₂CH(CH₃)CH₂), 21.18 (s, CHCH(CH₃)₂), 20.85 (s, CHCH(CH₃)₂), 15.65 (s, CHCH(CH₃)₂), 15.59 (s, CHCH(CH₃)₂). ³¹P{¹H} NMR (CDCl₃): δ 100.71 (br s). ¹¹B{¹H} NMR (CDCl₃): δ -39.48 (br s). Anal. Calcd for C₄₄H₆₀B₂O₃P₂: C, 73.35; H, 8.39. Found: C, 73.40; H, 8.38.

Synthesis of *rac*-2

To a solution of *rac*-1 (3.0 g, 4.16 mmol) in benzene (40 mL), MeLi (6.5 mL, 10.4 mmol, 1.6 M ether solution) was added dropwise. The reaction mixture was stirred at 40 °C for 14 h, and then 10 mL of water was added. The light brown solution became colourless upon addition of the water. The organic layer was separated and the aqueous solution was extracted with diethyl ether (2 × 10 mL). The combined organic fractions were washed with brine and dried over MgSO₄. The solution was concentrated and *rac*-2 was crystallized and isolated by filtration. Hexanes was added to the mother liquid and a second crop of crystals was obtained (combined yield: 1.08 g, 2.45 mmol, 59%). X-ray quality single crystals were obtained from layering hexanes onto a benzene solution of *rac*-2. ¹H NMR (CDCl₃): δ 8.19 (d, ³J_{HH} = 7.8 Hz, 2H, 1,9-dbf), 8.04 (dd, ³J_{HH} = 7.8 Hz, ³J_{PH} = 13.0 Hz, 2H, 3,7-dbf), 7.56–7.36 (ov m, 12H, 2,8-dbf + Ph), 1.59 (d, ²J_{PH} = 10.5 Hz, 6H, CH₃), 1.50–0.40 (br m, 6H, BH₃). ¹³C{¹H} NMR (CDCl₃): δ 156.68 (d, ²J_{CP} = 2.3 Hz, dbf-OC), 134.10 (d, ²J_{CP} = 13.6 Hz, *o*-Ph), 131.24 (d, ³J_{CP} = 2.3 Hz, *m*-Ph), 131.02 (d, ²J_{CP} = 9.8 Hz, 3,7-dbf), 130.16 (s, dbf), 129.16 (d, ²J_{CP} = 10.6 Hz, aromatic C), 125.14 (d, ²J_{CP} = 2.3 Hz, aromatic C), 124.18 (d, ²J_{CP} = 10.5 Hz, aromatic C), 124.06 (s, aromatic C), 113.57 (d, ¹J_{CP} = 52.8 Hz, 4,6-dbf), 10.54 (d, ¹J_{CP} = 40.0 Hz, CH₃). ³¹P{¹H} NMR (CDCl₃): δ 9.08 (br s). ¹¹B{¹H} NMR (CDCl₃): δ -37.21 (br s). Anal. Calcd for C₂₆H₂₈B₂O₂P₂: C, 70.96; H, 6.41. Found: C, 70.64; H, 6.38.

Identification of the by-product **3**: When the reaction was conducted at 23 °C and worked up as described above, column separation yielded *rac*-2 (for same scale as above, 0.73 g, 1.66 mmol, 40%) and the mono-methylated compound **3** (0.24 g, 0.42 mmol, 10%). X-ray quality single crystals were obtained from layering hexanes onto a benzene solution of **3**. Structural details are contained within the ESI† CIF file. ¹H NMR (CDCl₃): δ 8.26–8.19 (m, 2H, dbf), 8.12–8.09 (m, 1H, dbf), 7.96–7.89 (m, 1H, dbf), 7.71–7.65 (m, 2H, dbf/Ph), 7.61–7.27 (ov m, 10H, dbf/Ph), 4.34 (m, 1H, POCH-Men ring), 2.12 (d, ³J_{HH} = 12.0 Hz, 1H, OMen), 1.87 (d, ²J_{PH} = 10.8 Hz, 3H, PCH₃), 1.67–1.37 (ov m, 8H, OMen), 1.12 (q, ³J_{HH} = 12.0 Hz, 2H, OMen), 0.97–0.81 (ov m, 7H, OMen + BH₃), 0.61 (d, ³J_{HH} = 6.9 Hz, 3H, CH(CH₃)₂), 0.34 (d, ³J_{HH} = 6.9 Hz, 3H, CH(CH₃)₂). ¹³C{¹H} NMR (CDCl₃): δ 156.82 (d, ²J_{CP} = 3.0 Hz, dbf-OC), 155.71 (br s, dbf-OC), 133.82 (d, ²J_{CP} = 3.0 Hz, 3/7-dbf), 133.00 (s, dbf), 132.75 (d, ²J_{CP} = 12.1 Hz, 3/7-dbf), 131.98 (d, ⁴J_{CP} = 2.3 Hz, *p*-Ph), 131.68 (d, ²J_{CP} = 9.8 Hz, *o*-Ph), 131.22 (d, ⁴J_{CP} = 2.3 Hz, *p*-Ph), 130.99 (d, ²J_{CP} = 12.1 Hz, *o*-Ph), 130.26 (d, ¹J_{CP} = 75.5 Hz, *ipso*-Ph), 129.03 (d, ³J_{CP} = 10.6 Hz, 2/8-dbf), 128.86 (d, ³J_{CP} = 10.6 Hz, 2/8-dbf), 125.32

(d, ⁴J_{CP} = 2.3 Hz 1/9-dbf), 124.44 (d, ⁴J_{CP} = 2.3 Hz, 1/9-dbf), 124.25 (d, ³J_{CP} = 4.5 Hz, dbf), 124.09 (d, ³J_{CP} = 10.6 Hz, *m*-Ph), 123.89 (s, aromatic C), 123.74 (d, ³J_{CP} = 10.6 Hz, *m*-Ph), 116.92 (d, ¹J_{CP} = 61.9 Hz, 4/6-dbf), 114.16 (d, ¹J_{CP} = 52.8 Hz, 4/6-dbf), 80.82 (d, ²J_{CP} = 3.0 Hz, POCH-menthyl ring), 49.13 (d, ³J_{CP} = 6.0 Hz, CHCH(CH₃)₂), 43.82 (s, OCHCH₂CH), 34.22 (s, CH₃CHCH₂CH₂CH), 31.72 (s, CH₂CH(CH₃)CH₂), 25.46 (s, CHCH(CH₃)₂), 22.77 (s, CH₃CHCH₂CH₂CH), 22.28 (CH₂CH(CH₃)CH₂), 21.12 (s, CHCH(CH₃)₂), 15.20 (s, CHCH(CH₃)₂), 11.10 (d, ¹J_{CP} = 41.5 Hz, PCH₃). ³¹P{¹H} NMR (CDCl₃): δ 100.40 (br s), 8.65 (br s). ¹¹B{¹H} NMR (CDCl₃): δ -38.39 (br s). Anal. Calcd for C₃₅H₄₄B₂O₂P₂: C, 72.44; H, 7.64. Found: C, 72.05; H, 7.44.

Synthesis of *meso*-2

Meso-2 was prepared *via* a similar procedure as that described for *rac*-2, from *meso*-1 (2.9 g, 4 mmol) and MeLi (1.6 M in ether, 5.53 mL, 8.85 mmol) to afford a colourless solid (0.9 g, 2.0 mmol, 51%). ¹H NMR (CDCl₃): δ 8.14 (d, ³J_{HH} = 7.7 Hz, 2H, 1,9-dbf), 7.79–7.65 (ov m, 6H, *m*-Ph + *p*-Ph), 7.51–7.27 (ov m, 8H, *o*-Ph + 2,8-dbf + 3,7-dbf), 1.84 (d, ²J_{PH} = 10.4 Hz, 6H, PCH₃), 1.70–0.50 (br m, 6H, BH₃). ¹³C{¹H} NMR (CDCl₃): δ 156.73 (s, dbf-OC), 132.89 (d, ²J_{CP} = 9.9 Hz, *o*-Ph), 131.95 (d, ²J_{CP} = 9.9 Hz, 3,7-dbf), 131.61 (d, ³J_{CP} = 2.2 Hz, *m*-Ph), 129.77 (d, ¹J_{CP} = 57.4 Hz, *ipso*-Ph), 129.23 (d, ³J_{CP} = 10.5 Hz, 2,8-dbf), 124.63 (d, ⁴J_{CP} = 2.2 Hz, *p*-Ph), 124.22 (d, ⁴J_{CP} = 4.5 Hz, dbf), 124.05 (d, ³J_{CP} = 9.9 Hz, dbf), 114.58 (d, ¹J_{CP} = 52.8 Hz, 4,6-dbf), 11.37 (d, ¹J_{CP} = 40.8 Hz, CH₃). ³¹P{¹H} NMR (CDCl₃): δ 9.27 (br s). ¹¹B{¹H} NMR (CDCl₃): δ -37.65 (br s). Anal. Calcd for C₂₆H₂₈B₂O₂P₂: C, 70.96; H, 6.41. Found: C, 70.85; H, 6.40.

Synthesis of *rac*-4

Rac-2 (365 mg, 0.83 mmol) was suspended in diethylamine (15 mL) and the mixture was heated to 50 °C. After 2 h the solution was clear and colourless. After a total time of 15 h, the volatiles were removed under vacuum (9 × 10⁻³ torr) at 50 °C. Benzene (15 mL) was transferred to the reaction flask, then excess PippN₃ (401.4 mg, 2.49 mmol) was added. An immediate evolution of gas (presumably N₂) was observed. The light yellow solution was stirred at ambient temperature for 15 h and all volatiles were removed *in vacuo*. The residue was then heated to 100 °C under vacuum (9 × 10⁻³ torr) to remove the by-product Et₂NH·BH₃. Upon crystallization from benzene/pentane, pure *rac*-4 was obtained as a beige solid (380 mg, 0.56 mmol, 67%). ¹H NMR (CD₂Cl₂): δ 8.24 (d, ³J_{HH} = 7.7 Hz, 2H, 1,9-dbf), 8.09 (dd, ³J_{HH} = 7.6 Hz, ³J_{PH} = 12.8 Hz, 2H, 3,7-dbf), 7.55 (ov m, 8H, dbf + Ph), 7.41 (m, 4H, Ph), 6.84 (d, ³J_{HH} = 7.9 Hz, 4H, *m*-Pipp), 6.57 (d, ³J_{HH} = 8.1 Hz, 4H, *o*-Pipp), 2.72 (sp, ³J_{HH} = 6.9 Hz, 2H, CH(CH₃)₂), 1.73 (d, ²J_{PH} = 13.2 Hz, 6H, PCH₃), 1.14 (d, ³J_{HH} = 6.9 Hz, 12H, CH(CH₃)₂). ¹³C{¹H} NMR (CD₂Cl₂): δ 155.79 (d, ²J_{CP} = 3.3 Hz, dbf-OC), 149.35 (d, ³J_{CP} = 3.3 Hz, dbf-quaternary), 138.11 (s, *p*-Pipp), 133.49 (d, ²J_{CP} = 6.1 Hz, 3,7-dbf), 132.54 (d, ¹J_{CP} = 95.9 Hz, *ipso*-Ph), 132.34 (d, ³J_{CP} = 2.7 Hz, 2,8-dbf), 131.23 (d, ³J_{CP} = 9.9 Hz, *m*-Ph), 129.46 (d, ²J_{CP} = 12.1 Hz, *o*-Ph), 127.14 (d, ⁴J_{CP} = 1.1

Hz, *m*-Pipp), 125.42 (d, $^4J_{CP} = 3.0$ Hz, 1,9-dbf), 124.54 (s, *ipso*-Pipp), 124.40 (d, $^4J_{CP} = 9.8$ Hz, *p*-Ph), 122.88 (d, $^3J_{CP} = 18.7$ Hz, *o*-Pipp), 116.54 (d, $^1J_{CP} = 88.3$ Hz, 4,6-dbf), 33.67 (s, CH(CH₃)₂), 24.57 (s, CH(CH₃)₂), 14.91 (d, $^1J_{CP} = 78.5$ Hz, PCH₃). $^{31}\text{P}\{^1\text{H}\}$ NMR (CD₂Cl₂): δ -2.26 (s). Anal. Calcd for C₄₄H₄₄N₂OP₂: C, 77.86; H, 6.53; N, 4.13. Found: C, 77.39; H, 6.71; N, 4.08.

Synthesis of *rac*-4a

Rac-2 (400 mg, 0.91 mmol) was dissolved in diethylamine (10 mL) and heated to 50 °C for 17 h. All volatiles were removed *in vacuo* at 9×10^{-3} torr and an oily residue was obtained. Benzene (15 mL) was added, followed by slow addition of DippN₃ (462.5 mg, 2.25 mmol). Gas evolution was immediately observed. The light yellow solution was stirred for 12 h at ambient temperature, then all volatiles were removed *in vacuo*, yielding a light yellow residue. Pentane (10 mL) was added and the suspension was stirred, followed by filtration and washing with pentane to yield an off-white solid (470 mg, 0.62 mmol, 68%). X-ray quality single crystals were obtained from layering heptane onto a methylene chloride solution of *rac*-4a. ^1H NMR (CD₂Cl₂): δ 8.29 (dd, $^3J_{HH} = 7.5$ Hz, $^5J_{PH} = 1.2$ Hz, 1H, 1-dbf), 8.24 (d, $^3J_{HH} = 7.5$ Hz, 3H, 9 + 3,7-dbf), 7.59 (dt, $^3J_{HH} = 7.8$ Hz, $^4J_{PH} = 1.5$ Hz, 2H, 2,8-dbf), 7.47–7.30 (ov m, 10H, Ph), 6.90 (d, $^3J_{HH} = 7.5$ Hz, 4H, *m*-dipp), 6.72 (td, $^3J_{HH} = 7.5$ Hz, $^6J_{PH} = 2.1$ Hz, 2H, *p*-dipp), 3.15 (sp, $^3J_{HH} = 6.9$ Hz, 4H, CHMe₂), 1.55 (d, $^3J_{PH} = 12.6$ Hz, 6H, PCH₃), 0.96 (d, $^3J_{HH} = 6.9$ Hz, 12H, CHMe₂), 0.86 (d, $^3J_{HH} = 6.9$ Hz, 12H, CHMe₂). $^{13}\text{C}\{^1\text{H}\}$ NMR (CD₂Cl₂): δ 155.62 (d, $^2J_{CP} = 5.3$ Hz, dbf-OC), 144.39 (s, *o*-dipp), 143.09 (d, $^2J_{CP} = 6.8$ Hz, *ipso*-dipp), 135.22 (d, $^1J_{CP} = 95.8$ Hz, *ipso*-Ph), 133.20 (d, $^3J_{CP} = 3.8$ Hz, *m*-Ph), 131.72 (d, $^4J_{CP} = 2.3$ Hz, *p*-Ph), 130.42 (d, $^2J_{CP} = 10.6$ Hz, 3,8-dbf), 129.17 (d, $^2J_{CP} = 12.1$ Hz, *o*-Ph), 124.89 (s, *p*-dipp), 124.36 (d, $^3J_{CP} = 6.8$ Hz, quaternary dbf), 124.05 (d, $^3J_{CP} = 9.0$ Hz, 2,8-dbf), 122.93 (d, $^4J_{CP} = 1.5$ Hz, *m*-dipp), 119.57 (d, $^4J_{CP} = 3.0$ Hz, 1,9-dbf), 118.60 (d, $^1J_{CP} = 109.4$ Hz, 4,6-dbf), 28.84 (s, CH(CH₃)₂), 24.00 (s, CH(CH₃)₂), 23.78 (s, CH(CH₃)₂), 15.84 (d, $^1J_{CP} = 69.4$ Hz, PCH₃). $^{31}\text{P}\{^1\text{H}\}$ NMR (CD₂Cl₂): δ -15.21 (s). Anal. Calcd for C₅₀H₅₆N₂OP₂: C, 78.71; H, 7.40; N, 3.67. Found: C, 78.68; H, 7.68; N, 3.77.

Synthesis of *meso*-4

Meso-4 was prepared *via* a similar procedure as that described for *rac*-4. Thus, *meso*-2 (283 mg, 0.643 mmol), diethylamine (15 mL) and PippN₃ (238.5 mg, 1.48 mmol), yielded a colourless solid (310 mg, 0.46 mmol, 71%). ^1H NMR (CD₂Cl₂): δ 8.20 (d, $^3J_{HH} = 7.8$ Hz, 2H, 1,9-dbf), 7.90 (dd, $^3J_{HH} = 7.6$ Hz, $^3J_{PH} = 12.7$ Hz, 2H, 3,7-dbf), 7.76 (dd, $^3J_{HH} = 7.6$ Hz, $^3J_{PH} = 12.3$ Hz, 4H, *m*-Ph), 7.53–7.36 (ov m, 8H, 2,8-dbf + *o*-Ph + *p*-Ph), 6.84 (d, $^3J_{HH} = 8.1$ Hz, 4H, *m*-Pipp), 6.59 (d, $^3J_{HH} = 8.1$ Hz, 4H, *o*-Pipp), 2.72 (sp, $^3J_{HH} = 6.9$ Hz, 2H, CH(CH₃)₂), 2.08 (d, $^2J_{PH} = 13.2$ Hz, 6H, PCH₃), 1.14 (d, $^3J_{HH} = 6.9$ Hz, 12H, CH(CH₃)₂). $^{13}\text{C}\{^1\text{H}\}$ NMR (CD₂Cl₂): δ 156.28 (d, $^2J_{CP} = 2.7$ Hz, dbf-OC), 149.55 (d, $^2J_{CP} = 3.3$ Hz, *ipso*-Pipp), 137.97 (s, *p*-Pipp), 133.04 (s, quaternary dbf), 132.78 (d, $^2J_{CP} = 6.1$ Hz, 3,7-dbf), 132.25 (d, $^4J_{CP} = 2.8$ Hz, *p*-Ph), 131.59 (d, $^3J_{CP} = 10.5$

Hz, *m*-Ph), 129.34 (d, $^2J_{CP} = 12.1$ Hz, *o*-Ph), 127.16 (s, *m*-Pipp), 125.25 (d, $^4J_{CP} = 2.2$ Hz, 1,9-dbf), 124.65 (d, $^1J_{CP} = 6.1$ Hz, *ipso*-Ph), 124.25 (d, $^3J_{CP} = 9.5$ Hz, 2,8-dbf), 122.92 (d, $^3J_{CP} = 19.3$ Hz, *o*-Pipp), 117.19 (d, $^1J_{CP} = 85.3$ Hz, 4,6-dbf), 33.67 (s, CH(CH₃)₂), 24.58 (s, CH(CH₃)₂), 15.35 (d, $^1J_{CP} = 74.3$ Hz, PCH₃). $^{31}\text{P}\{^1\text{H}\}$ NMR (CD₂Cl₂): δ -2.07 (s). Anal. Calcd for C₄₄H₄₄N₂OP₂: C, 77.86; H, 6.53; N, 4.13. Found: C, 77.42; H, 6.54; N, 4.20.

Synthesis of *rac*-5a

Rac-4a (200 mg, 0.26 mmol) and [H(Et₂O)₂]⁺[B(3,5-{CF₃})₂C₆H₃)₄][−] (265 mg, 0.26 mmol) were dissolved in benzene (3 mL) and the yellowish solution was stirred for 1 h. Volatiles were removed *in vacuo* and pentane (5 mL) was added to the residue. The resultant colourless solid was collected by filtration and washed with pentane (2 × 5 mL) (390 mg, 0.24 mmol, 91%). X-ray quality single crystals were obtained from layering heptane onto a methylene chloride solution of *rac*-5a. ^1H NMR (CD₂Cl₂): δ 8.38 (d, $^3J_{HH} = 7.8$ Hz, 2H, 1,9-dbf), 7.85–7.68 (ov m, 16H, 3,7-dbf + *o*-C₆H₃(CF₃)₂-Ph), 7.55 (s, 4H, *p*-C₆H₃(CF₃)₂), 7.42–7.36 (br m, 2H, *p*-dipp), 7.19 (br m, 4H, *m*-Ph), 7.07 (br ov m, 6H, *m*-dipp + *p*-dipp), 4.79 (br s, 1H, NH), 2.81 (sp, $^3J_{HH} = 6.6$ Hz, 4H, CHMe₂), 2.00 (d, $^2J_{PH} = 12.3$ Hz, 6H, PCH₃), 0.92 (d, $^3J_{HH} = 6.6$ Hz, 12H, CHMe₂), 0.66 (d, $^3J_{HH} = 6.6$ Hz, 12H, CHMe₂). $^{13}\text{C}\{^1\text{H}\}$ NMR (CD₂Cl₂): δ 162.29 (q, 1 : 1 : 1 : 1, $^1J_{BC} = 49.8$ Hz, *ipso*-B[C₆H₃(CF₃)₂]₄), 156.41 (s, dbf-OC), 145.60 (br ov, *ipso*-dipp and *o*-dipp), 135.34 (s, *o*-C₆H₃(CF₃)₂), 134.30 (br, *p*-dipp), 131.00 (d, $^3J_{CP} = 11.3$ Hz, *m*-Ph), 130.45 (ov, *ipso*-Ph), 130.28 (d, $^2J_{CP} = 13.6$ Hz, *o*-Ph), 129.40 (qq, $^2J_{CF} = 31.4$ Hz, $^3J_{CB} = 2.7$ Hz, *m*-C₆H₃(CF₃)₂), 129.39 (ov, quaternary dbf), 127.58 (br s, 1,9-dbf), 125.52 (d, $^2J_{CP} = 10.6$ Hz, 3,7-dbf), 125.14 (q, $^1J_{CF} = 272.5$ Hz, CF₃), 124.75 (d, $^3J_{CP} = 6.0$ Hz, 2,8-dbf), 124.42 (br s, *m*-dipp and *p*-Ph), 118.02 (br sp, $^3J_{CF} = 4.5$ Hz, *p*-C₆H₃(CF₃)₂), 29.39 (s, CH(CH₃)₂), 24.00 (s, CH(CH₃)₂), 23.41 (s, CH(CH₃)₂), 10.96 (d, $^3J_{CP} = 66.6$ Hz, PCH₃). One aromatic carbon signal was not observed. $^{31}\text{P}\{^1\text{H}\}$ NMR (CD₂Cl₂): δ 9.17 (br s). $^{11}\text{B}\{^1\text{H}\}$ NMR (CD₂Cl₂): δ -6.61 (s). $^{19}\text{F}\{^1\text{H}\}$ NMR (CD₂Cl₂): δ -62.83 (s). Anal. Calcd for C₈₂H₆₉BF₂₄N₂OP₂: C, 60.53; H, 4.27; N, 1.72. Found: C, 60.75; H, 4.26; N, 1.89.

Synthesis of *rac*-5b

Rac-5b was prepared *via* a similar procedure as that described for *rac*-5a from *rac*-4a (208 mg, 0.27 mmol) and [H(Et₂O)₂]⁺[B(C₆F₅)₄][−] (210 mg, 0.27 mmol) to afford a colourless solid (380 mg, 0.26 mmol, 96.6%). ^1H NMR (CD₂Cl₂): δ 8.41 (d, $^3J_{HH} = 7.8$ Hz, 2H, 1,9-dbf), 7.90–7.68 (ov m, 8H, dbf + Ph), 7.42 (br t, $^3J_{HH} = 7.5$ Hz, 2H, aromatic H), 7.21 (br ov m, 4H, aromatic H), 7.07 (br ov m, 6H, dipp), 4.78 (br s, 1H, NH), 2.82 (sp, $^3J_{HH} = 6.6$ Hz, 4H, CH(CH₃)₂), 1.98 (d, $^3J_{PH} = 12.3$ Hz, 6H, PCH₃), 0.92 (d, $^3J_{HH} = 6.8$ Hz, 12H, CH(CH₃)₂), 0.68 (d, $^3J_{HH} = 6.8$ Hz, 12H, CH(CH₃)₂). $^{13}\text{C}\{^1\text{H}\}$ NMR (CD₂Cl₂): δ 156.41 (s, dbf-OC), 150.31 (br, aromatic quaternary C), 147.12 (br, aromatic quaternary C), 145.65 (br, aromatic quaternary C), 140.47 (br m, B(C₆F₅)₄), 138.34 (br m, B(C₆F₅)₄), 137.14 (br m, B(C₆F₅)₄), 135.14 (br m, B(C₆F₅)₄), 134.43 (br s, Ph), 131.70

(ov, aromatic C), 131.02 (d, J_{CP} = 6.6 Hz, aromatic C), 130.30 (d, J_{CP} = 12.8 Hz, aromatic C), 128.85 (s, aromatic C), 127.68 (br s, 1,9-dbf), 127.65 (ov, aromatic C), 125.56 (d, J_{CP} = 10.6 Hz, aromatic C), 124.83 (br s, aromatic quaternary C), 124.43 (s, dipp), 29.40 (s, $CH(CH_3)_2$), 23.98 (s, $CH(CH_3)_2$), 23.42 (s, $CH(CH_3)_2$), 10.94 (br d, J_{CP} = 74.0 Hz, PCH_3). $^{31}P\{^1H\}$ NMR (CD_2Cl_2): δ 9.2 (br). $^{11}B\{^1H\}$ NMR (CD_2Cl_2): δ -16.67 (s). $^{19}F\{^1H\}$ NMR (CD_2Cl_2): δ -133.08 (br, 8F, *o*- C_6F_5), -163.62 (t, J_{FF} = 21.2 Hz, 4F, *p*- C_6F_5), -167.48 (br, 8F, *m*- C_6F_5). Anal. Calcd for $C_{74}H_{57}BF_{20}N_2OP_2$: C, 61.59; H, 3.98; N, 1.94. Found: C, 60.70; H, 4.00; N, 2.19.

Synthesis of *rac*-5

Rac-5 was prepared via a similar procedure as that described for *rac*-5a, using *rac*-4 (345 mg, 0.508 mmol) and $[H(Et_2O)_2]^+ [B(3,5-(CF_3)_2C_6H_3)_4]^-$ (515 mg, 0.508 mmol) to obtain a colourless solid (680 mg, 0.44 mmol, 87%). 1H NMR (CD_2Cl_2): δ 8.34 (d, J_{HH} = 7.6 Hz, 2H, 1,9-dbf), 7.73–7.45 (ov m, 26H, dbf + Ph + $C_6H_3(CF_3)_2$), 6.91 (d, J_{HH} = 7.9 Hz, 4H, *m*-Pipp), 6.62 (d, J_{HH} = 8.1 Hz, 4H, *o*-Pipp), 6.42 (br s, 1H, NH), 2.74 (sp, J_{HH} = 6.9 Hz, 2H, $CH(CH_3)_2$), 2.09 (d, J_{PH} = 12.9 Hz, 6H, PCH_3), 1.12 (d, J_{HH} = 6.8 Hz, 12H, $CH(CH_3)_2$). $^{13}C\{^1H\}$ NMR (CD_2Cl_2): δ 162.33 (q 1:1:1:1, J_{BC} = 49.8 Hz, *ipso*-B [$C_6H_3(CF_3)_2$]₄), 156.92 (s, dbf-OC), 143.36 (s, *p*-Pipp), 141.50 (s, quaternary dbf), 135.36 (s, *o*- $C_6H_3(CF_3)_2$), 134.60 (d, J_{CP} = 2.8 Hz, *p*-Ph), 132.18 (d, J_{CP} = 7.5 Hz, 3,7-dbf), 132.04 (d, J_{CP} = 11.3 Hz, *m*-Ph), 130.24 (d, J_{CP} = 13.2 Hz, *o*-Ph), 129.42 (qq, J_{CF} = 31.79 Hz, J_{CB} = 3.0 Hz, *m*- $C_6H_3(CF_3)_2$), 128.03 (s, *m*-Pipp), 127.78 (d, J_{CP} = 2.8 Hz, 1,9-dbf), 125.99 (d, J_{CP} = 107.17 Hz, *ipso*-Ph), 125.45 (d, J_{CP} = 10.4 Hz, *o*-Pipp), 125.14 (q, J_{CF} = 272.5 Hz, CF_3), 124.79 (d, J_{CP} = 10.4 Hz, *ipso*-Pipp), 123.33 (d, J_{CP} = 12.8 Hz, 2,8-dbf), 118.03 (sp, J_{CF} = 3.9 Hz, *p*- $C_6H_3(CF_3)_2$), 112.13 (d, J_{CP} = 90.8 Hz, 4,6-dbf), 33.81 (s, $CH(CH_3)_2$), 24.28 (s, $CH(CH_3)_2$), 13.06 (d, J_{CP} = 71.7 Hz, PCH_3). $^{31}P\{^1H\}$ NMR (CD_2Cl_2): δ 15.20 (s). $^{11}B\{^1H\}$ NMR (CD_2Cl_2): δ -6.57 (s). $^{19}F\{^1H\}$ NMR (CD_2Cl_2): δ -61.89 (s). Anal. Calcd for $C_{76}H_{57}BF_{24}N_2OP_2$: C, 59.16; H, 3.72; N, 1.82. Found: C, 59.27; H, 3.87; N, 1.91.

Synthesis of *meso*-5

Meso-5 was prepared via a similar procedure as that described for *rac*-5a, from *meso*-4 (240 mg, 0.354 mmol) and $[H(Et_2O)_2]^+ [B(3,5-(CF_3)_2C_6H_3)_4]^-$ (358 mg, 0.354 mmol) to yield a beige solid (440 mg, 0.29 mmol, 81%). 1H NMR (CD_2Cl_2): δ 8.35 (d, J_{HH} = 7.4 Hz, 2H, 1,9-dbf), 7.73–7.36 (m, 26H, dbf + Ph + $C_6H_3(CF_3)_2$), 6.89 (d, J_{HH} = 8.3 Hz, 4H, *m*-Pipp), 6.62 (d, J_{HH} = 7.9 Hz, 4H, *o*-Pipp), 6.39 (br s, 1H, NH), 2.73 (sp, J_{HH} = 6.9 Hz, 2H, $CH(CH_3)_2$), 2.17 (d, J_{PH} = 13.0 Hz, 6H, PCH_3), 1.12 (d, J_{HH} = 6.8 Hz, 12H, $CH(CH_3)_2$). $^{13}C\{^1H\}$ NMR (CD_2Cl_2): δ 162.30 (q, 1:1:1:1, J_{BC} = 49.8 Hz, *ipso*-B [$C_6H_3(CF_3)_2$]₄), 157.04 (s, dbf-OC), 143.35 (s, *p*-Pipp), 141.58 (s, quaternary dbf), 135.34 (s, *o*- $C_6H_3(CF_3)_2$), 134.55 (d, J_{CP} = 2.8 Hz, *p*-Ph), 131.98 (d, J_{CP} = 10.6 Hz, *o*-Ph), 131.94 (d, J_{CP} = 4.5 Hz, 3,7-dbf), 130.18 (d, J_{CP} = 13.2 Hz, *m*-Ph), 129.42 (qq, J_{CF} = 30.9 Hz, J_{CB} = 2.8 Hz, *m*- $C_6H_3(CF_3)_2$), 128.86 (s, *ipso*-Ph), 127.96 (s, *m*-Pipp), 127.76 (br, 1,9-dbf), 125.44 (d,

J_{CP} = 9.8 Hz, 2,8-dbf), 125.14 (q, J_{CF} = 272.5 Hz, CF_3), 124.77 (d, J_{CP} = 6.0 Hz, *ipso*-Pipp), 123.68 (d, J_{CP} = 12.7 Hz, *o*-Pipp), 118.03 (sp, J_{CF} = 3.87 Hz, *p*- $C_6H_3(CF_3)_2$), 112.37 (d, J_{CP} = 89.1 Hz, 4,6-dbf), 33.80 (s, $CH(CH_3)_2$), 24.28 (s, $CH(CH_3)_2$), 12.95 (d, J_{CP} = 70.9 Hz, PCH_3). $^{31}P\{^1H\}$ NMR (CD_2Cl_2): δ 15.84 (s). $^{11}B\{^1H\}$ NMR (CD_2Cl_2): δ -6.60 (s). $^{19}F\{^1H\}$ NMR (CD_2Cl_2): δ -61.93 (s). Anal. Calcd for $C_{76}H_{57}BF_{24}N_2OP_2$: C, 59.16; H, 3.72; N, 1.82. Found: C, 59.60; H, 3.74; N, 1.91.

Synthesis of *rac*-6

Rac-5 (100 mg, 64.8 μ mol) was dissolved in methylene chloride (1.5 mL) and excess diethylzinc (0.1 mL) was added. The solution was stirred at ambient temperature for 15 min and the volatiles were removed *in vacuo*. After washing with pentane (3 \times 2 mL), the thick residue was dried under reduced pressure to give a white solid (100 mg, 60.9 μ mol, 94%). 1H NMR (CD_2Cl_2): δ 8.37 (d, J_{HH} = 7.7 Hz, 2H, 1,9-dbf), 7.72–7.45 (ov m, 26H, dbf + Ph + $C_6H_3(CF_3)_2$), 6.80 (d, J_{HH} = 8.0 Hz, 4H, *m*-Pipp), 6.48 (d, J_{HH} = 8.0 Hz, 4H, *o*-Pipp), 2.74 (sp, J_{HH} = 6.9 Hz, 2H, $CH(CH_3)_2$), 2.14 (d, J_{PH} = 12.7 Hz, 6H, PCH_3), 1.14 (d, J_{HH} = 7.0 Hz, 12H, $CH(CH_3)_2$), 0.64 (t, J_{HH} = 8.0 Hz, 3H, CH_3CH_2Zn), -0.22 (q, J_{HH} = 8.0 Hz, 2H, CH_3CH_2Zn). $^{13}C\{^1H\}$ NMR (CD_2Cl_2): δ 162.29 (q 1:1:1:1, J_{BC} = 50.0 Hz, *ipso*-B [$C_6H_3(CF_3)_2$]₄), 156.73 (s, dbf-OC), 144.48 (d, J_{CP} = 3.0 Hz, *p*-Pipp), 142.80 (d, J_{CP} = 6.0 Hz, quaternary dbf), 135.35 (s, *o*- $C_6H_3(CF_3)_2$), 134.56 (d, J_{CP} = 2.8 Hz, *p*-Ph), 131.99 (d, J_{CP} = 10.6 Hz, *o*-Ph), 130.76 (d, J_{CP} = 8.3 Hz, 3,7-dbf), 130.17 (d, J_{CP} = 12.7 Hz, *m*-Ph), 129.42 (qq, J_{CF} = 30.9 Hz, J_{CB} = 2.3 Hz, *m*- $C_6H_3(CF_3)_2$), 127.93 (d, J_{CP} = 1.5 Hz, 1,9-dbf), 127.55 (d, J_{CP} = 101.0 Hz, *ipso*-Ph), 126.90 (ov *m*-Pipp), 126.26 (d, J_{CP} = 11.0 Hz, *o*-Pipp), 125.86 (d, J_{CP} = 9.9 Hz, 2,8-dbf), 125.15 (q, J_{CF} = 272.5 Hz, CF_3), 124.74 (d, J_{CP} = 6.1 Hz, *ipso*-Pipp), 118.02 (sp, J_{CF} = 4.0 Hz, *p*- $C_6H_3(CF_3)_2$), 113.64 (d, J_{CP} = 101.9 Hz, 4,6-dbf), 33.84 (s, $CH(CH_3)_2$), 24.29 (s, $CH(CH_3)_2$), 13.05 (d, J_{CP} = 67.9 Hz, PCH_3), 12.55 (s, CH_3CH_2Zn), 2.23 (s, CH_3CH_2Zn). $^{31}P\{^1H\}$ NMR (CD_2Cl_2): δ 24.98 (s). $^{11}B\{^1H\}$ NMR (CD_2Cl_2): δ -6.61 (s). $^{19}F\{^1H\}$ NMR (CD_2Cl_2): δ -61.95 (s). Anal. Calcd for $C_{78}H_{61}BF_{24}N_2OP_2Zn$: C, 57.25; H, 3.76; N, 1.71. Found: C, 57.44; H, 3.88; N, 1.78.

Synthesis of *rac*-6a

In a glovebox, *rac*-5a (60 mg, 0.0369 mmol) was dissolved in bromobenzene (0.5 mL), and diethylzinc (excess) was added dropwise. After stirring the solution for 5 min, pentane (3 mL) was added and an oil formed in the bottom of the reaction vessel. The pentane layer was separated and the oil was washed with pentane (3 \times 3 mL), yielding a solid which was dried *in vacuo* (50 mg, 0.029 mmol, 78.9%). X-ray quality single crystals were obtained from layering heptane onto a methylene chloride solution of *rac*-6a. 1H NMR (CD_2Cl_2): δ 8.43 (d, J_{HH} = 7.8 Hz, 2H, 1,9-dbf), 7.72 (br ov m, 10H, dbf + Ph), 7.55 (br ov m, 8H, Ph + B [$C_6H_3(CF_3)_2$]₄), 7.41–7.27 (br m, 8H, B [$C_6H_3(CF_3)_2$]₄), 7.13 (m, 2H, *p*-dipp), 7.00 (br m, 4H, *m*-dipp), 3.05 (br m, 4H, $CH(CH_3)_3$), 2.08 (d, J_{PH} = 11.4 Hz, 6H, PCH_3), 0.90–0.30 (br

m, 24H, CH(CH₃)₃), 0.01 (t, ³J_{HH} = 7.8 Hz, 3H, ZnCH₂CH₃), −0.80 (br m, 2H, ZnCH₂CH₃). ¹³C{¹H} NMR (CD₂Cl₂): δ 162.29 (q, 1 : 1 : 1 : 1, ¹J_{BC} = 49.8 Hz, *ipso*-B[C₆H₃(CF₃)₂]₄), 157.41 (s, dbf-OC), 146.16 (d, ³J_{CP} = 4.8 Hz, dbf-quaternary), 135.33 (s, *o*-C₆H₃(CF₃)₂), 134.29 (br s, *p*-Ph), 132.11 (br ov m, *o*-Ph + dbf), 130.34 (ov, dbf), 130.14 (d, ²J_{CP} = 12.8 Hz, *m*-Ph), 129.38 (qq, ²J_{CF} = 31.9 Hz, ³J_{CB} = 2.7 Hz, *m*-C₆H₃(CF₃)₂), 127.51 (d, ⁴J_{CP} = 2.2 Hz, 1,9-dbf), 126.35 (d, ³J_{CP} = 2.6 Hz, *o*-dipp), 125.99 (d, ³J_{CP} = 10.6 Hz, 2,8-dbf), 125.43 (s, *p*-dipp), 125.12 (q, ¹J_{CF} = 272.5 Hz, CF₃), 124.68 (d, ²J_{CP} = 6.8 Hz, *ipso*-dipp), 124.34 (d, ¹J_{CP} = 101.1 Hz, *ipso*-Ph), 118.02 (sp, ³J_{CF} = 4.0 Hz, *p*-C₆H₃(CF₃)₂), 115.33 (d, ¹J_{CP} = 100.0 Hz, 4,6-dbf), 28.93 (s, CH(CH₃)₂), 24.74 (s, CH(CH₃)₂), 13.28 (d, ¹J_{CP} = 167.5 Hz, PCH₃), 6.57 (s, CH₂CH₃), −0.05 (s, CH₂CH₃). ³¹P{¹H} NMR (CD₂Cl₂): δ 24.49 (br s). ¹¹B{¹H} NMR (CD₂Cl₂): δ −6.61 (s). ¹⁹F{¹H} NMR (CD₂Cl₂): δ −62.84 (s). Anal. Calcd for C₈₄H₇₃BF₂₄N₂OP₂Zn: C, 58.64; H, 4.28; N, 1.63. Found: C, 58.15; H, 4.24; N, 1.57.

Synthesis of *rac*-6b

Rac-6b was prepared via a similar procedure as that described for *rac*-6a (using *rac*-5b, 76.0 mg, 0.05 mmol) to afford a white solid (74.4 mg, 4.84 mmol, yield 92%). ¹H NMR (CD₂Cl₂): δ 8.44 (d, ³J_{HH} = 7.8 Hz, 2H, 1,9-dbf), 7.69 (dt, ³J_{HH} = 7.8 Hz, ³J_{PH} = 2.4 Hz, 2H, 2,8-dbf), 7.63–7.46 (br ov m, 4H, Ph), 7.46–7.20 (br ov m, 8H, dbf + Ph), 7.13 (dt, ³J_{HH} = 7.5 Hz, ⁶J_{PH} = 2.1 Hz, 2H, *p*-dipp), 7.01 (br ov m, 4H, *m*-dipp), 3.06 (br m, 4H, CH(CH₃)₂), 2.08 (d, ²J_{PH} = 11.4 Hz, 6H, PCH₃), 1.20–0.18 (br ov m, 24H, CH(CH₃)₂), 0.01 (t, ³J_{HH} = 8.1 Hz, 3H, ZnCH₂CH₃), −0.79 (br m, 2H, ZnCH₂CH₃). ¹³C{¹H} NMR (CD₂Cl₂): δ 157.40 (s, dbf-OC), 150.24 (br, aromatic C), 147.15 (br, aromatic C), 146.26 (s, aromatic C), 141.11 (br, B(C₆F₅)₄), 140.39 (br, B(C₆F₅)₄), 138.49 (br, B(C₆F₅)₄), 136.98 (br, B(C₆F₅)₄), 135.17 (br, aromatic C), 134.27 (s, aromatic C), 132.24 (br, aromatic C), 130.15 (d, ²J_{CP} = 12.8 Hz, *o*-Ph), 127.55 (s, 1,9-dbf), 126.34 (s, aromatic C), 126.00 (d, ⁴J_{CP} = 10.6 Hz, *m*-dipp), 125.41 (s, 2,8-dbf), 124.74 (s, aromatic C), 115.32 (d, ¹J_{CP} = 96.6 Hz, 4,6-dbf), 28.93 (s, CH(CH₃)₂), 24.73 (s, CH(CH₃)₂), 14.63 (d, ¹J_{CP} = 36.2 Hz, PCH₃), 12.16 (s, CH₃CH₂Zn), 6.57 (s, CH₃CH₂Zn). ³¹P{¹H} NMR (CD₂Cl₂): δ 24.65 (br s). ¹¹B{¹H} NMR (CD₂Cl₂): δ −16.67 (s). ¹⁹F{¹H} NMR (CD₂Cl₂): δ −133.05 (br, 8F, *o*-C₆F₅), −163.69 (t, ³J_{FF} = 19.7 Hz, 4F, *p*-C₆F₅), −167.53 (br, 8F, *m*-C₆F₅). Anal. Calcd for C₇₆H₆₁BF₂₀N₂OP₂Zn: C, 59.41; H, 4.00; N, 1.82. Found: C, 58.39; H, 4.00; N, 1.78.

Synthesis of *meso*-6

Meso-6 was prepared via a similar procedure as that described for *rac*-6, using *meso*-5 (100 mg, 64.8 μmol) and diethylzinc (0.05 mL, excess), yielding a white solid (94 mg, 57.7 μmol, 89%). ¹H NMR (CD₂Cl₂): δ 8.42 (d, ³J_{HH} = 7.9 Hz, 2H, 1,9-dbf), 7.73–7.52 (ov m, 22H, dbf + Ph + C₆H₃(CF₃)₂), 7.42 (m, 4H, *m*-Ph), 6.76 (d, ³J_{HH} = 8.1 Hz, 4H, *m*-Pipp), 6.44 (dd, ³J_{HH} = 8.5 Hz, ³J_{PH} = 2.1 Hz, 4H, *o*-Pipp), 2.71 (sp, ³J_{HH} = 6.8 Hz, 2H, CH(CH₃)₂), 2.17 (d, ²J_{PH} = 12.7 Hz, 6H, PCH₃), 1.12 (d, ³J_{HH} = 6.8 Hz, 12H, CH(CH₃)₂), 0.68 (t, ³J_{HH} = 8.1 Hz, 3H,

CH₃CH₂Zn), −0.33 (q, ³J_{HH} = 8.1 Hz, 2H, CH₃CH₂Zn). ¹³C{¹H} NMR (CD₂Cl₂): δ 162.30 (q 1 : 1 : 1 : 1, ¹J_{BC} = 49.6 Hz, *ipso*-B[C₆H₃(CF₃)₂]₄), 156.78 (s, dbf-OC), 144.57 (d, ⁵J_{CP} = 3.3 Hz, *p*-Pipp), 142.69 (d, ³J_{CP} = 6.0 Hz, quaternary dbf), 135.34 (s, *o*-C₆H₃(CF₃)₂), 134.42 (d, ⁴J_{CP} = 2.8 Hz, *p*-Ph), 131.78 (d, ³J_{CP} = 10.5 Hz, *m*-Ph), 130.74 (d, ²J_{CP} = 8.3 Hz, 3,7-dbf), 130.11 (d, ²J_{CP} = 12.7 Hz, *o*-Ph), 129.40 (qq, ²J_{CF} = 31.3 Hz, ³J_{CB} = 2.8 Hz, *m*-C₆H₃(CF₃)₂), 128.14 (d, ¹J_{CP} = 104.0 Hz, *ipso*-Ph), 127.85 (br ov, 1,9-dbf and *m*-Pipp), 126.25 (d, ³J_{CP} = 11.6 Hz, *o*-Pipp), 125.99 (d, ³J_{CP} = 9.4 Hz, 2,8-dbf), 125.12 (q, ¹J_{CF} = 272.5 Hz, CF₃), 124.80 (d, ²J_{CP} = 5.3 Hz, *ipso*-Pipp), 118.01 (sp, ³J_{CF} = 4.5 Hz, *p*-C₆H₃(CF₃)₂), 113.52 (d, ¹J_{CP} = 101.1 Hz, 4,6-dbf), 33.79 (s, CH(CH₃)₂), 24.27 (s, CH(CH₃)₂), 12.59 (s, CH₃CH₂Zn), 12.11 (d, ¹J_{CP} = 67.1 Hz, PCH₃), 2.58 (s, CH₃CH₂Zn). ³¹P{¹H} NMR (CD₂Cl₂): δ 24.98 (s). ¹¹B{¹H} NMR (CD₂Cl₂): δ −6.61 (s). ¹⁹F{¹H} NMR (CD₂Cl₂): δ −61.96 (s). Anal. Calcd for C₇₈H₆₁BF₂₄N₂OP₂Zn: C, 57.25; H, 3.76; N, 1.71. Found: C, 57.37; H, 3.81; N, 1.77.

Synthesis of *rac*-7

Rac-7 was prepared via a similar procedure as that described for *rac*-6, from *rac*-5 (100 mg, 64.8 μmol) and dimethylzinc (1.2 M toluene solution, 0.27 mL) to yield a beige solid (84 mg, 51.84 μmol, 80%). ¹H NMR (CD₂Cl₂): δ 8.40 (dt, ³J_{HH} = 7.9 Hz, ⁵J_{PH} = 1.3 Hz, 2H, 1,9-dbf), 7.72–7.41 (ov m, 26H, dbf + Ph + C₆H₃(CF₃)₂), 6.80 (d, ³J_{HH} = 7.9 Hz, 4H, *m*-Pipp), 6.47 (dd, ³J_{HH} = 8.4 Hz, ⁴J_{PH} = 2.2 Hz, 4H, *o*-Pipp), 2.74 (sp, ³J_{HH} = 6.9 Hz, 2H, CH(CH₃)₂), 2.13 (d, ²J_{PH} = 12.5 Hz, 6H, PCH₃), 1.14 (d, ³J_{HH} = 6.9 Hz, 12H, CH(CH₃)₂), −1.10 (s, 3H, ZnCH₃). ¹³C{¹H} NMR (CD₂Cl₂): δ 162.36 (q 1 : 1 : 1 : 1, ¹J_{BC} = 49.7 Hz, *ipso*-B[C₆H₃(CF₃)₂]₄), 156.73 (s, dbf-OC), 144.65 (d, ⁵J_{CP} = 3.3 Hz, *p*-Pipp), 142.61 (d, ³J_{CP} = 6.6 Hz, quaternary dbf), 135.35 (s, *o*-C₆H₃(CF₃)₂), 134.53 (d, ⁴J_{CP} = 3.3 Hz, *p*-Ph), 132.03 (d, ²J_{CP} = 10.5 Hz, *o*-Ph), 130.95 (d, ²J_{CP} = 7.7 Hz, 3,7-dbf), 130.11 (d, ²J_{CP} = 12.7 Hz, *m*-Ph), 129.41 (qq, ²J_{CF} = 31.9 Hz, ³J_{CB} = 2.9 Hz, *m*-C₆H₃(CF₃)₂), 128.86 (s, *m*-Pipp), 127.86 (d, ⁴J_{CP} = 1.7 Hz, 1,9-dbf), 127.58 (d, ¹J_{CP} = 102.4 Hz, *ipso*-Ph), 126.20 (d, ³J_{CP} = 11.3 Hz, *o*-Pipp), 126.14 (d, ³J_{CP} = 9.1 Hz, 2,8-dbf), 125.15 (q, ¹J_{CF} = 272.5 Hz, CF₃), 124.77 (d, ²J_{CP} = 6.0 Hz, *ipso*-Pipp), 118.03 (sp, ³J_{CF} = 3.8 Hz, *p*-C₆H₃(CF₃)₂), 113.46 (d, ¹J_{CP} = 101.1 Hz, 4,6-dbf), 33.85 (s, CH(CH₃)₂), 24.30 (s, CH(CH₃)₂), 13.14 (d, ¹J_{CP} = 68.7 Hz, PCH₃), −11.75 (s, CH₃Zn). ³¹P{¹H} NMR (CD₂Cl₂): δ 25.71 (s). ¹¹B{¹H} NMR (CD₂Cl₂): δ −6.61 (s). ¹⁹F{¹H} NMR (CD₂Cl₂): δ −61.95 (s). Anal. Calcd for C₇₇H₅₉BF₂₄N₂OP₂Zn: C, 57.00; H, 3.67; N, 1.73. Found: C, 57.13; H, 3.77; N, 1.79.

Synthesis of *meso*-7

Meso-7 was prepared via a similar procedure as that described for *meso*-6, from *meso*-5 (100 mg, 64.8 μmol) and dimethylzinc (excess, 324 μmol, 1.2 M toluene solution, 0.27 mL) to yield a beige solid (103 mg, 63.5 μmol, 98%). ¹H NMR (CD₂Cl₂): δ 8.44 (d, ³J_{HH} = 7.9 Hz, 2H, 1,9-dbf), 7.72 (br ov m, 10H, *o*-Ph + *p*-Ph + dbf), 7.60–7.48 (ov m, 12H, C₆H₃(CF₃)₂), 7.40 (m, 4H, *m*-Ph), 6.74 (d, ³J_{HH} = 8.3 Hz, 4H, *m*-Pipp), 6.42 (dd, ³J_{HH} = 8.5 Hz, ³J_{PH} = 2.0 Hz, 4H, *o*-Pipp), 2.70 (sp, ³J_{HH} = 6.9 Hz,

Table 3 Selected crystal and refinement data for compounds *rac-1*, *meso-1*, *rac-2*, **3**, *rac-4a*, *rac-5a*, *rac-5b*, *rac-6a*, *meso-6* and *meso-7*

	<i>rac-1</i> ·0.67 (C ₅ H ₁₂)	<i>meso-1</i>	<i>rac-2</i>	3	<i>rac-4a</i>	<i>rac-5a</i>	<i>rac-5b</i>	<i>rac-6a</i>	<i>meso-6</i>	<i>meso-7</i>
Chemical Formula	C _{47.33} H ₆₈ B ₂ O ₃ P ₂	C ₄₉ H ₇₂ B ₂ O ₃ P ₂	C ₂₆ H ₂₈ B ₂ OP ₂	C ₃₅ H ₄₄ B ₂ O ₂ P ₂	C ₅₃ H ₅₉ N ₂ OP ₂	C ₈₂ H ₆₉ BF ₂₄ N ₂ OP ₂	C ₇₄ H ₅₇ BF ₂₀ N ₂ OP ₂	C ₈₅ H ₇₅ BCl ₂ F ₂₄ N ₂ OP ₂ Zn	C ₇₈ H ₆₁ BF ₂₄ N ₂ OP ₂ Zn	C ₇₇ H ₅₉ BF ₂₄ N ₂ O P ₂ Zn
Formula Weight	768.58	792.67	440.04	580.26	801.96	1627.14	1442.97	1805.49	1636.41	1622.38
Crystal System	Monoclinic	Monoclinic	Monoclinic	Monoclinic	Triclinic	Monoclinic	Monoclinic	Monoclinic	Triclinic	Triclinic
Space Group	<i>P</i> 2 ₁	<i>P</i> 2 ₁	<i>P</i> 2 ₁	<i>P</i> 2 ₁	<i>P</i> $\bar{1}$	<i>P</i> 2 ₁ / <i>n</i>	<i>P</i> 2 ₁ / <i>n</i>	<i>P</i> 2 ₁ / <i>n</i>	<i>P</i> $\bar{1}$	<i>P</i> $\bar{1}$
<i>a</i> /Å	12.0455(15)	9.1131(6)	9.0916(15)	8.866(2)	10.682(3)	25.9495(19)	17.8759(16)	23.695(3)	15.008(3)	15.1464(9)
<i>b</i> /Å	9.0733(11)	17.7459(11)	26.778(5)	15.561(4)	12.265(4)	15.9645(12)	19.0247(17)	16.3001(17)	15.591(3)	15.4468(9)
<i>c</i> /Å	21.256(3)	15.5104(10)	10.3509(17)	12.610(3)	18.315(6)	39.031(3)	39.597(4)	23.842(3)	16.299(3)	16.3669(9)
α (°)	90	90	90	90	102.736(4)	90	90	90	89.306(2)	88.5290(10)
β (°)	96.742(2)	102.5560(10)	106.329(2)	109.266(2)	93.563(4)	103.7470(10)	99.0010(10)	114.8180(10)	76.703(2)	76.3750(10)
γ (°)	90	90	90	90	103.759(4)	90	90	90	85.884(2)	86.1190(10)
<i>V</i> /Å ³	2307.0(5)	2448.4(3)	2418.3(7)	1642.3(6)	2256.7(12)	15706(2)	13301(2)	8358.1(15)	3701.7(11)	3712.8(4)
<i>Z</i>	2	2	4	2	2	8	8	4	2	2
GOF on <i>F</i> ²	0.891	0.933	1.191	1.059	0.928	0.972	0.840	1.095	1.029	1.085
Refined Data/Parameters	10776/468	10818/468	11011/567	7512/376	10280/533	36047/2239	30607/1786	19174/1214	16897/1017	16850/1092
<i>R</i> ₁ [<i>I</i> > 2σ(<i>I</i>)] ^a	0.0862	0.0352	0.0617	0.0289	0.0401	0.0563	0.0611	0.0568	0.0652	0.0463
w <i>R</i> ₂ {all data} ^a	0.2275	0.0765	0.1403	0.0857	0.0967	0.1685	0.1839	0.1610	0.2149	00.1398
Flack parameter	−0.08(15)	0.00(4)	0.44(11)	0.03(5)						

^a *R*₁ = Σ||*F*_o| − |*F*_c||/Σ |*F*_o|; w*R*₂ = [Σw(*F*_o² − *F*_c²)/Σw(*F*_o²)]^{1/2}.

2H, CH(CH₃)₂), 2.12 (d, ²J_{PH} = 12.5 Hz, 6H, PCH₃), 1.12 (d, ³J_{HH} = 6.9 Hz, 12H, CH(CH₃)₂), -1.22 (s, 3H, CH₃Zn). ¹³C {¹H} NMR (CD₂Cl₂): δ 162.31 (q 1 : 1 : 1 : 1, ¹J_{BC} = 49.8 Hz, *ipso*-B[C₆H₃(CF₃)₂]₄), 156.96 (s, dbf-OC), 144.69 (s, *p*-Pipp), 142.60 (d, ³J_{CP} = 4.9 Hz, quaternary dbf), 135.35 (s, *o*-C₆H₃(CF₃)₂), 134.46 (s, *p*-Ph), 132.00 (d, ³J_{CP} = 11.2 Hz, *m*-Ph), 130.99 (d, ²J_{CP} = 8.3 Hz, 3,7-dbf), 130.05 (d, ²J_{CP} = 12.7 Hz, *o*-Ph), 129.51 (qq, ²J_{CF} = 31.3 Hz, ³J_{CB} = 3.2 Hz, *m*-C₆H₃(CF₃)₂), 127.86 (d, ¹J_{CP} = 107.7 Hz, *ipso*-Ph), 127.82 (br ov, 1,9-dbf and *m*-Pipp), 126.14 (d, ³J_{CP} = 9.4 Hz, *o*-Pipp), 125.14 (q, ¹J_{CF} = 272.5 Hz, CF₃), 124.82 (d, ²J_{CP} = 6.0 Hz, 2,8-dbf), 124.51 (d, ²J_{CP} = 54.0 Hz, *ipso*-Pipp), 118.03 (sp, ³J_{CF} = 4.2 Hz, *p*-C₆H₃(CF₃)₂), 113.32 (d, ¹J_{CP} = 98.9 Hz, 4,6-dbf), 33.82 (s, CH(CH₃)₂), 24.29 (s, CH(CH₃)₂), 12.34 (d, ¹J_{CP} = 67.9 Hz, PCH₃), -10.97 (s, CH₃Zn). ³¹P {¹H} NMR (CD₂Cl₂): δ 25.57 (s). ¹¹B {¹H} NMR (CD₂Cl₂): δ -6.61 (s). ¹⁹F {¹H} NMR (CD₂Cl₂): δ -61.97 (s). Anal. Calcd for C₇₇H₅₉BF₂₄N₂OP₂Zn: C, 57.00; H, 3.67; N, 1.73. Found: C, 57.07; H, 3.69; N, 1.69.

NMR scale polymerisation of *rac*-lactide with *rac*-6 and *meso*-6

In a glovebox, *rac*-lactide (72.1 mg, 0.5 mmol) and an appropriate amount of initiator (*e.g.* M/I = 200, 4.1 mg, 2.5 μmol) were dissolved in CDCl₃ (0.5 mL) in an NMR tube. The tube was sealed with a rubber septum, and placed in an oil bath (40 °C). The polymerisation was monitored every 30 min until >95% conversion was observed by ¹H NMR spectroscopy. These conditions were then used for the large scale polymerisation reactions. For determination of activation parameters, data were recorded at the appropriate temperatures, which were corrected by using the equation $T_{\text{actual}} = 1.111T_0 - 1.8505$.

Large scale polymerisation of *rac*-lactide with *rac*-6 and *meso*-6

In a glovebox, *rac*-lactide (144.1 mg, 1 mmol) and an appropriate amount of initiator (*e.g.* M/I = 200, 8.2 mg) were dissolved in methylene chloride (1 mL) in a scintillation vial. The solution was stirred for an appropriate period of time (using NMR scale conditions). This yielded a thick glue-like substance. In air, the crude product was washed with cold methanol (2 × 5 mL), and dried *in vacuo* (9 × 10⁻³ torr) yielding the solid polymer.

X-ray crystallographic studies

X-ray crystallography. A high quality crystal of each compound was coated in Paratone oil and mounted on a glass fiber. Data were collected at low temperature (173 K) with ω and ϕ scans on a Bruker Smart Apex II diffractometer using graphite-monochromated Mo-K α radiation ($\lambda = 0.71073$ Å) and Bruker SMART software.²⁵ Unit cell parameters were calculated and refined from the full data set. Cell refinement and data reduction were performed using the Bruker APEX2 and SAINT programs, respectively.²⁶ Reflections were scaled and corrected for absorption effects using SADABS.²⁷ The structures were solved by direct methods with SHELXS²⁸ and refined by full-matrix least-squares techniques against F^2 using SHELXL.²⁹ All non-hydrogen atoms were refined anisotropically. All hydrogen atoms (except the N–H atoms, which were located from the electron

density maps and refined freely) were placed in calculated positions and refined using a riding model.

Crystal data are summarized in Table 3. No special considerations were required for the refinement of the compounds, except *rac*-1, in which disordered pentane solvent molecules were present. The electron density related to the molecule was removed using SQUEEZE.³⁰ Some of the crystals featured disordered organic substituents, in particular the fluorinated borate anions. Where possible these groups were modelled isotropically over two positions, although in a few cases no suitable model could be found, resulting in large thermal displacement parameters.

Conclusions

In summary, a new series of P-stereogenic neutral bisphosphinimine ligands, and cationic alkylzinc complexes thereof, have been synthesized and fully characterised. The successful diastereomeric resolution of these ligands represents an advancement in the dbf ligand design, as the monophosphinimine derivatives formed inseparable *rac/meso* mixtures. Two complexes in particular, *rac*-6 and *meso*-6, were shown to initiate the ring-opening polymerisation of *rac*-lactide to yield polymer samples with a modest heterotactic bias and with significantly higher activity than our first-generation initiators. Although significant *trans*-esterification side reactions led to high polydispersity indices, high conversion was attained. Furthermore, while mechanistic details remain elusive, kinetic data suggest that *rac*-6 and *meso*-6 are in fact pre-catalysts, which react in solution to form the active species. To help test this hypothesis, future studies will focus on the preparation of hydroxy, alkoxide and lactate derivatives of the alkylzinc complexes presented herein and investigations of their competency as catalysts for PLA synthesis. To improve the stereocontrol of polymerisation, future ligand variants may incorporate larger chiral groups to increase steric differentiation. In addition, placement of the chiral functionality closer to the metal centre (*e.g.* on nitrogen rather than phosphorus) is also anticipated to enhance chiral induction.

Acknowledgements

The authors wish to acknowledge financial support from NSERC (Canada), Canada Foundation for Innovation, Canada School of Energy and Environment and GreenCentre Canada. Thanks are given to Dr. Craig Wheaton for performing elemental analyses of new compounds, Mr. Tony Montina for expert technical assistance, GreenCentre Canada for GPC analysis, and the Mass Spectrometric Facility at the Department of Chemistry, University of Alberta, for MALDI-TOF characterization of PLA samples.

References

‡ Due to the chiral mentholate substituents on phosphorus, the terms *rac*- and *meso*- are not strictly accurate. However, for simplicity we make use of these descriptors in reference to the relative stereochemistry of the two chiral phosphorus sites in each stereoisomer. The two isomers are also denoted as (*R,R,R,R*) and (*R,S,S,R*) in-text, where the first and last *R*'s refer to the stereochemistry of the carbon centre in the OMen group closest to the phosphorus atom.

- 1 J. Ahmed and S. K. Varshney, *Int. J. Food Prop.*, 2011, **14**, 37–58.
- 2 B. D. Ulery, L. S. Nair and C. T. Laurencin, *J. Polym. Sci., Part B: Polym. Phys.*, 2011, **49**, 832–864.
- 3 (a) *US Pat.*, 5 258 488, 1993; (b) *US Pat.*, 6 143 863, 2000.
- 4 P. J. Dijkstra, H. Du and J. Feijen, *Polym. Chem.*, 2011, **2**, 520–527.
- 5 C. A. Wheaton, P. G. Hayes and B. J. Ireland, *Dalton Trans.*, 2009, 4823–4846.
- 6 (a) M. H. Chisholm, J. C. Gallucci and K. Phomphrai, *Inorg. Chem.*, 2005, **44**, 8004–8010; (b) A. P. Dove, V. C. Gibson, E. L. Marshall, A. J. P. White and D. J. Williams, *Dalton Trans.*, 2004, 570–578; (c) M. H. Chisholm, J. C. Huffinan and K. Phomphrai, *J. Chem. Soc., Dalton Trans.*, 2001, 222–224; (d) M. Cheng, A. B. Attygalle, E. B. Lobkovsky and G. W. Coates, *J. Am. Chem. Soc.*, 1999, **121**, 11583–11584.
- 7 (a) V. Poirier, T. Roisnel, J.-F. Carpentier and Y. Sarazin, *Dalton Trans.*, 2009, 9820–9827; (b) Z. Zheng, G. Zhao, R. Fablet, M. Bouyahyi, C. M. Thomas, T. Roisnel, O. Casagrande and J.-F. Carpentier, *New J. Chem.*, 2008, **32**, 2279–2291; (c) W.-C. Hung, Y. Huang and C.-C. Lin, *J. Polym. Sci., Part A: Polym. Chem.*, 2008, **46**, 6466–6476; (d) J. Ejfler, S. Szafert, K. Mierzwicki, L. B. Jerzykiewicz and P. Sobota, *Dalton Trans.*, 2008, 6556–6562; (e) L. E. Breyfogle, C. K. Williams, V. G. Young, M. A. Hillmyer and W. B. Tolman, *Dalton Trans.*, 2006, 928–936; (f) C. K. Williams, N. R. Brooks, M. A. Hillmyer and W. B. Tolman, *Chem. Commun.*, 2002, 2132–2133; (g) V. Poirier, T. Roisnel, J.-F. Carpentier and Y. Sarazin, *Dalton Trans.*, 2011, **40**, 523–534; (h) Y. Sarazin, V. Poirier, T. Roisnel and J.-F. Carpentier, *Eur. J. Inorg. Chem.*, 2010, 3423–3428.
- 8 (a) M. H. Chisholm, N. W. Eilerts, J. C. Huffman, S. S. Iyer, M. Pacold and K. Phomphrai, *J. Am. Chem. Soc.*, 2000, **122**, 11845–11854; (b) M. H. Chisholm, *Inorg. Chim. Acta*, 2009, **362**, 4284–4290.
- 9 (a) Y. Sarazin, B. Liu, T. Roisnel, L. Maron and J.-F. Carpentier, *J. Am. Chem. Soc.*, 2011, **133**, 9069–9087. For related examples of dications stabilized by monoanionic ligands, see: (b) M. G. Cushion and P. Mountford, *Chem. Commun.*, 2011, **47**, 2276–2278; (c) E. Piedra-Arroni, P. Brignou, A. Amgoune, S. M. Guillaume, J.-F. Carpentier and D. Bourissou, *Chem. Commun.*, 2011, **47**, 9828–9830.
- 10 B. J. Ireland, C. A. Wheaton and P. G. Hayes, *Organometallics*, 2010, **29**, 1079–1084.
- 11 (a) C. A. Wheaton, B. J. Ireland and P. G. Hayes, *Organometallics*, 2009, **28**, 1282–1285; (b) C. A. Wheaton and P. G. Hayes, *Dalton Trans.*, 2010, **39**, 3861–3869; (c) C. A. Wheaton and P. G. Hayes, *Chem. Commun.*, 2010, **46**, 8404–8406; (d) C. A. Wheaton and P. G. Hayes, *Catal. Sci. Technol.*, 2012, **2**, 125–138.
- 12 (a) Y. Ikada, K. Jamshidi, H. Tsuji and S.-H. Hyon, *Macromolecules*, 1987, **20**, 904–906; (b) K. Fukushima and Y. Kimura, *Polym. Int.*, 2006, **55**, 626–642.
- 13 (a) L. Zhang, F. Nederberg, J. M. Messman, R. C. Pratt, J. L. Hedrick and C. G. Wade, *J. Am. Chem. Soc.*, 2007, **129**, 12610–12611; (b) J. A. Byers and J. E. Bercaw, *Proc. Natl. Acad. Sci. U. S. A.*, 2006, **103**, 15303–15308.
- 14 H. Sun, J. S. Ritch and P. G. Hayes, *Inorg. Chem.*, 2011, **50**, 8063–8072.
- 15 M. W. Haenel, D. Jakubik, E. Rothenberger and G. Schroth, *Chem. Ber.*, 1991, **124**, 1705–1710.
- 16 (a) H. Staudinger and J. Meyer, *Helv. Chim. Acta*, 1919, **2**, 635–646; (b) M. Alajarin, C. Lopez-Leonardo, P. Llamas-Lorente and D. Bautista, *Synthesis*, 2000, 2085–2091.
- 17 F. Drouin, P. O. Oguadinma, T. J. J. Whitehorne, R. E. Prud'homme and F. Schaper, *Organometallics*, 2010, **29**, 2139–2147.
- 18 (a) A. Bondi, *J. Phys. Chem.*, 1964, **68**, 441–452; (b) B. Cordero, V. Gómez, A. E. Platero-Prats, M. Revés, J. Echeverría, E. Cremades, F. Barragán and S. Alvarez, *Dalton Trans.*, 2008, 2832–2838.
- 19 (a) A. F. Douglas, B. O. Patrick and P. Mehrkhodavandi, *Angew. Chem., Int. Ed.*, 2008, **47**, 2290–2293; (b) M. H. Chisholm, J. C. Gallucci and C. Krempner, *Polyhedron*, 2007, **26**, 4436–4444; (c) M. H. Chisholm and E. E. Delbridge, *New J. Chem.*, 2003, **27**, 1177–1183.
- 20 E. B. Schwartz, C. B. Knobler and D. J. Cram, *J. Am. Chem. Soc.*, 1992, **114**, 10775–10784.
- 21 M. Brookhart, B. Grant and A. F. Volpe, *Organometallics*, 1992, **11**, 3920–3922.
- 22 P. Jutzi, C. Müller, A. Stammler and H.-G. Stammler, *Organometallics*, 2000, **19**, 1442–1444.
- 23 L. P. Spencer, R. Altwer, P. Wei, L. Gelmini, J. Gauld and D. W. Stephan, *Organometallics*, 2003, **22**, 3841–3854.
- 24 K. R. D. Johnson and P. G. Hayes, *Organometallics*, 2009, **28**, 6352–6361.
- 25 *APEX 2, Crystallography software package*, Bruker AXS Inc., Madison, WI, 2005.
- 26 *SAINT, Data Reduction Software*, Bruker AXS, 1999.
- 27 G. M. Sheldrick, *SADABS v.2.01, Area Detector Absorption Correction Program*, Bruker AXS, Madison, WI, 1998.
- 28 G. M. Sheldrick, *SHELXS-97, Program for solution of crystal structures*, University of Göttingen, Göttingen, Germany, 1997.
- 29 G. M. Sheldrick, *SHELXL-97, Program for refinement of crystal structures*, University of Göttingen, Göttingen, Germany, 1997.
- 30 P. Van Sluis and A. L. Spek, *Acta Crystallogr., Sect. A: Found. Crystallogr.*, 1990, **46**, 194–201.